Review and detailed analysis of the Plio-Quaternary tectono-stratigraphic architecture and evolution of the Sicily Channel (Central Mediterranean)

Nicolò Chizzini[1]*, Mariagiada Maiorana[2], Aasiya Qadir[1], Eline Le Breton[3], Mimmo Palano[2], Andrea Artoni[1], Alina Polonia[4], Luca Gasperini[4], Attilio Sulli[2], Luigi Torelli[1]

[1] Department of Chemistry, Life Sciences and Environmental Sustainability University of Parma, Parco Area delle Scienze, 157/A, Parma, Italy

[2] Department of Earth and Marine Sciences, University of Palermo, Via Archirafi 22, 90123 Palermo, Italy

[3] Univ Rennes, CNRS, Géosciences Rennes - UMR 6118, Rennes, France

[4] Institute of Marine Sciences CNR ISMAR-Bo, Via Gobetti, 101, 40129 Bologna, Italy

*Corresponding author: nicolo.chizzini@unipr.it

Keywords: Sicily Channel; Central Mediterranean; Foreland tectonics; inversion tectonics; Strike-slip tectonics; Rifting zone

Abstract

The regions outward the leading edge of the orogenic wedges and external to the associated foredeep basin, i.e., the foreland areas, are often perceived as stable zones. Nevertheless the Sicily Channel—situated in the central Mediterranean between Sicily and Tunisia and regarded as the continental foreland of the Sicilian Maghrebian chain—reveals significant tectonic complexity. It comprises three major tectonic troughs (Pantelleria, Malta, and Linosa grabens) formed by the ongoing extension of Africa. This area includes a foreland-foredeep-mountain chain system encompassing the Pelagian foreland, the Gela Foredeep Basin, and the offshore section of the Neogene-Quaternary Sicilian-Maghrebian chain. Based on an extensive review of available literature, including previously published multichannel seismic reflection profiles and structural maps, we provide a detailed analysis of the stratigraphic architecture and key

This provisional PDF is the accepted version. The article should be cited as: BSGF - Earth Sciences Bulletin, https://doi.org/10.1051/bsgf/2025018

tectonic features in the Sicily Channel during the Plio-Quaternary. Furthermore, we assess the timing of major tectonic events to gain a comprehensive understanding of the region's Plio-Quaternary structural evolution. Our findings demonstrate that the Sicily Channel is not merely a simple rifted foreland zone but is characterized by recurrent extensional and compressional phases during the late Neogene/Plio-Quaternary. This evidence indicates that distinct tectonic regimes can spatially and temporally coexist within a foreland area, reinforcing the idea that foreland zones actively record dynamic processes driving lithospheric deformation and are prone to tectonic reactivation.

French résumé

Bien que les régions d'avant-pays soient souvent perçues comme des zones tectoniques stables, le canal de Sicile - situé en Méditerranée centrale entre la Sicile et la Tunisie et considéré comme l'avant-pays continental de la chaîne maghrébo-sicilienne - révèle une complexité tectonique importante. Cette zone comprend trois fossés tectoniques (Pantelleria, Malta et Linosa grabens), formés par l'extension de la plaque Afrique, ainsi qu'un système compressif comprenant l'avant-pays pélagien, le bassin d'avant-pays de Gela et la partie offshore de la chaîne maghrébo-sicilienne néo-quaternaire. D'après un examen approfondi de la littérature disponible, y compris des profils de réflexion sismique multicanaux et des cartes structurales publiés précédemment, nous présentons une analyse détaillée de l'architecture stratigraphique et des principales caractéristiques tectoniques qui ont influencé le canal de Sicile depuis la fin du Miocène. En outre, nous évaluons la chronologie de ces événements afin d'acquérir une compréhension globale de l'évolution tectonique Plio-Quaternaire de la région. Nos résultats montrent que le canal de Sicile n'est pas simplement une simple zone

d'avant-pays rifté, mais qu'il est caractérisé par des phases d'extension et de compression récurrentes au cours fin du Miocène et du Plio-Quaternaire. Ces données indiquent que des régimes tectoniques distincts peuvent coexister dans une zone d'avant-pays, renforçant l'idée que ces zones enregistrent activement les processus dynamiques à l'origine de la déformation lithosphérique régionale et sont susceptibles d'être réactivées tectoniquement.

1. Introduction

Forelands bordering foredeep basins (*sensu DeCelles and Giles, 1996*) commonly considered as the areas ahead of the orogens not affected by shortening processes, are key tectonic elements in the periphery of orogenic belts, forming as an indirect response to continental underthrusting (*Allen et al., 1986; Allen and Allen, 1990; Cloetingh et al., 1994; Ziegler et al., 1994, 1995; DeCelles and Giles, 1996; DeCelles, 2012; Cloething et al., 2015; Royden and Faccenna, 2018*). In the central Mediterranean, the Sicily Channel is part of the African continental foreland, lying south of the Maghrebian–Apenninic/Sicilian orogenic system. Despite its foreland classification, the region displays notable tectonic complexity and active deformation (*Civile et al., 2014; Cavallaro et al., 2017; Meccariello et al., 2017; Fedorik et al., 2018; Ferranti et al., 2019; Civile et al., 2021; Milia et al., 2021; Maiorana et al., 2023; Micallef et al., 2024; Civile et al., 2024*)

Over the past decedes, numerous marine campaigns and studies have been carried out in the Sicily Channel to determine the main tectonic structures affecting this region, their timing of activity, and ultimately suggesting a geological evolution for this area (*Finetti, 1984; Argnani et al., 1986; Antonelli et al., 1988; Lentini et al. 1990, 1994, 1996; Catalano et al., 1996, 2000; Finetti and Del Ben, 2005; Civile et al., 2008, 2010, 2014, 2016; Cavallaro et al., 2017; Meccariello et al.; 2017; Civile et al., 2018; Fedorik et al., 2018; Ferranti et al., 2019; Civile et al., 2021; Volpi et al., 2022; Maiorana et al., 2023*).

All the recent studies recognized the existence of both extensional and recent contractional structures in the Sicily Channel. The latter were believed to be positive inverted faults that enucleated from inherited Mesozoic extensional discontinuities. These structures were explained as being caused by the compressive stress exerted from the surrounding fold-and-thrust belts—such as the Egadi Thrust Front (ETF), the Gela Thrust System (GTS), and the Adventure Thrust Front (ATF) (Fig. 1)—during Plio-Quaternary, in the broader context of Africa–Eurasia convergence (Argnani et al., 1986; *Torelli et al., 1998*; *Holland et al., 2003; Corti et al., 2006; Civile et al., 2014; Meccariello et al., 2017; Civile et al., 2021; Cavallaro et al., 2017; Maiorana et al., 2023*). However, most previous studies have focused on isolated sectors of the Sicily Channel, and a region-wide synthesis remains lacking.

In this work, we present a comprehensive review and interpretation of existing seismic reflection profiles and structural data, with particular focus on key areas such as the offshore Capo-Granitola Sciacca Fault Zone (CGSFZ), the Adventure Plateau, as well as the frontal part of the GTS (Fig. 1), to provide a more comprehensive and updated structural map of the Sicily Channel and the surrounding areas. Furthermore, we analyze the Plio-Quaternary tectonic evolution of the region in relation to its Mesozoic paleogeographic inheritance. This broader perspective provides insights into the tectonic processes shaping the foreland and may serve as a comparative framework for other foreland regions worldwide.

This work aims at providing a unified and harmonized synthesis of previously published seismic profiles and structural data in the Sicily Channel to propose a consistent interpretative framework in distinguishing seismic sequences and regional unconformities. This integrated approach enables a coherent regional-scale view of the Sicily Channel and its geodynamic significance within the central Mediterranean context.

2. Geological setting of the Sicily Channel

2.1 Geographic location and tectonic background

The Sicily Channel is a wide, shallow-water platform that stretches across an area of approximately 250,000 km^2, located between Tunisia and Sicily in the northern part of the African continental plate, or the so-called Pelagian Block (Fig. 1) (*Burrollet et al., 1978; Argnani et al., 1986; Butler et al., 1992; Torelli et al., 1998; Lickorish et al., 1999; Holland et al., 2003; Corti et al., 2006; Civile et al., 2014; Cavallaro et al., 2017; Meccariello et al., 2017; Fedorik et al., 2018; Ferranti et al., 2019; Civile et al., 2021; Milia et al., 2021; Volpi et al., 2022; Maiorana et al., 2023, 2024; Micallef et al., 2024; Civile et al., 2024*). The Sicily Channel terminates at the West with the Adventure Plateau, and at the East with the Malta Plateau (Fig. 1).

The region was shaped by the Neogene NNW-directed convergence between the African and Eurasian plates that led to the closure of the Neo-Tethys Ocean and the progressive collision between the African and European continental margins (*Gueguen et al., 1998; Goes et al., 2004; Carminati et al., 2012; Civile et al., 2021*), resulting in the development of a typical collisional system with three major structural domains: the Sicilian–Maghrebian fold-and-thrust belt, the Gela Foredeep Basin, and the Pelagian foreland (*Cavallaro et al., 2017; Civile et al., 2021; Maiorana et al., 2023*).

The Pelagian foreland, which includes the study area, represents a relatively undeformed sector of the African continental margin. It is characterized by a thinned continental crust, ranging from 25 to 35 km in thickness, but locally reduced to about 17 km near Pantelleria Island due to continental rifting processes (*Burollet et al., 1978; Catalano et al., 1995*). To the north, the Gela Foredeep Basin basin forms a narrow, elongated Plio-Quaternary depocenter, developed due to flexural subsidence of the foreland beneath the advancing Sicilian-Maghrebian orogenic wedge. It hosts more than 2 km of clastic sediments and is spatially associated with the south-verging Gela Nappe, the outermost thrust sheet of the chain (*Cogan et al., 1989; Cavallaro et al., 2017*). West of the Gela Foredeep Basin lies the offshore sector of the Sicilian–Maghrebian fold-and-thrust belt, which includes the Adventure Plateau. This sector preserves a record of Miocene compressional phases, with ESE-verging thrusts belonging to the ETF and ATF domains, deform Tortonian–Messinian foredeep deposits (e.g., Terravecchia Fm.) and the Meso-Cenozoic carbonate basement (*Civile et al., 2014; Civile et al., 2021*).

The central part of the Sicily Channel is affected by Plio-Pleistocene continental rifting, leading to the formation of NW-trending, fault-bounded grabens (the Pantelleria, Linosa, and Malta grabens). A major lithospheric structure in the study region is the Capo-Granitola Sciacca Fault Zone, a NNE-trending strike-slip fault system that has been interpreted as a major transfer zone separating different tectonic domains of the chain. It extends for over 200 km from Linosa Island to the southern coast of Sicily and likely played a key role in the segmentation and development of the rift, possibly marking the boundary between the western Pantelleria and the eastern Linosa and Malta grabens (*Fedorik et al., 2018; Ferranti et al., 2019*) (Fig. 1).

2.2 Tectonic evolution

For a better understanding of the geodynamic setting of the Sicily Channel, it is essential to consider the tectonic evolution of the Central Mediterranean region. During the Mesozoic, African and Eurasian plate divergence led to the opening of the Alpine Tethys Ocean (*Catalano and D'Argenio, 1982; Jongsma et al., 1985; Stampfli et al., 2001; Stampfli, 2005; Handy et al.,* *2010; Van Hinsbergen et al., 2020; Le Breton et al., 2021; Critelli, and Martín-Martín, 2024*). This was followed by the progressive closure of the Alpine Tethys from the Cretaceous onward, which resulted in the fragmentation and reorganization of earlier paleogeographic domains (*Catalano and D'Argenio, 1982; Casero et al., 1984; Antonelli et al., 1988; Catalano et al., 2000; Basilone, 2009*). A second extensional event occurred during the Early Cretaceous, characterized by widespread rifting in the Sirte and Tripolitania Basins of Tunisia, and is interpreted as the expression of a broader extensional regime linked to Central African tectonics (*Stampfli et al., 2001*).

From the Late Cretaceous to the Middle Eocene, the Central Mediterranean experienced a NW–SE oriented compressive stress regime (*Antonelli et al., 1988; Torelli et al., 1995*), coinciding with a shift in African plate motion triggered by the opening of the South Atlantic ocean (*Stampfli and Borel, 2002; Stampfli, 2005; Handy et al., 2010; Van Hinsbergen et al., 2020; Le Breton et al., 2021*). Later, during the Late Oligocene to Early Miocene, rollback of the subducting slab in the western Mediterranean induced extension in the overriding plate, with the opening of the Liguro–Provencal Basin and a counterclockwise rotation of the Sardinia–Corsica block. This tectonic reorganization was coeval with the accretion of the Sicilian–Maghrebian fold-and-thrust belt (*Civile et al., 2021*) or Sicilian Fold-and-Thrust Belt (*Speranza et al., 2018*).

During the Messinian , the disconnection of the Mediterranean Sea to the Atlantic Ocean led to the Messinian Salinity Crisis, a significant event that impacted the paleogeographic and environmental evolution of the Mediterranean region, including the Sicily Channel (*Butler et al., 1995; Krijgsman et al., 1999; Butler, 2009; Lofi et al., 2011; Roveri et al., 2014; Aksu et al., 2018; Günes et al., 2018; Camerlenghi et al., 2020; Manzi et al., 2020, 2021; Pellen et al., 2022*).

This event led to a prominent sea-level drop probably in the order of hundreds of meters (*de Alteriis, 1995*) and the consequent emersion and erosion of a large part of the banks/seamounts of the Sicily Channel (*Civile et al., 2015; Cavallaro et al., 2017; Meccariello et al., 2017*), as well as the sedimentation of very thick, locally up to 3 km, evaporites in the deep Ionian Sea to the East (*Lofi et al., 2011; Roveri et al., 2014; Haq et al., 2020; Manzi et al., 2020, 2021*).

In the Late Miocene, the Sicily Channel was a foreland area with respect to the Sicilian-Maghrebian fold-and-thust belt (*Civile et al., 2021*) and it was characterized by the presence of several carbonate structural highs (e.g., Adventure Plateau, Nameless Bank, Linosa Plateau, Madrepore Bank, and Hyblean Plateau; Fig. 1); moreover, a strike-slip regime affected the Sicily Channel, and this is well documented at Lampedusa Island (*Grasso and Pedley, 1985; Meccariello et al., 2017*). A continental rift-related process, started since the Lower Pliocene and controlled by sub-vertical normal faults, led to the formation of the Malta, Linosa, and Pantelleria WNW-ESE-oriented elongate grabens (*Finetti, 1984; Boccaletti et al., 1987; Cello, 1987; Grasso and Torelli, 1999; Carminati and Doglioni, 2005; Catalano et al., 2009*; *Civile et al., 2010; Ghielmi et al., 2012; Cavallaro et al., 2017; Meccariello et al., 2017; Civile et al., 2021; Maiorana et al., 2023*). A passive rifting process is widely accepted as the main mechanism responsible for the graben’s origin and localized crustal thinning observed in the Sicily Channel (*Finetti, 1984; Civile et al., 2010; Civile et al., 2021*). Several authors have proposed that the extension was driven by two major dextral strike-slip fault systems, which promoted the formation of pull-apart basins (*Jongsma et al., 1985; Reuther and Eisbacher, 1985; Boccaletti et al., 1987; Catalano et al., 2009*). On the other hand, *Argnani (1990, 2009)* suggested that rifting was triggered by mantle convection associated with the roll-back and slab-pull of the African slab beneath the Tyrrhenian Basin. *Arab et al. (2020)* linked the extensional tectonics of the Sicily Channel to the presence of a Subduction-Transform Edge Propagator fault or to eastward-directed slab tearing segmenting the African slab and facilitating its retreat (*Govers and Wortel, 2005; Rosenbaum et al., 2008*). Finally, other authors (e.g., *Corti et al., 2006*) have suggested that the accretion of the Sicilian-Maghrebian fold-and-thurst belt and the rifting in the Sicily Channel represent two independent tectonic processes that acted synchronously. Changes in asthenospheric flows, along with this Lower Pliocene extensional tectonic phase, prompted the Moho to rise under the major grabens of Malta, Pantelleria, and Linosa, resulting in volcanic manifestations near the grabens' margins (*Maiorana et al., 2023; Bongiovanni et al., 2025*). The scattered anorogenic volcanism is mainly concentrated on the islands of Pantelleria and Linosa (*Rotolo et al., 2006*; *Civile et al., 2013; Micallef et al., 2024*), in the Adventure Plateau, and in the Sciacca offshore (*Peccerillo, 2005; Rotolo et al., 2006; Civile et al., 2013; Lodolo et al., 2019; Civile et al., 2024; Micallef et al., 2024*) (Fig. 2).

In the Lower-Upper Pliocene, the advance of the GTS triggered a first compressional tectonic phase, evidenced by the positive inversion of pre-existing extensional faults, especially in the Madrepore Graben (*Civile et al., 2021*; *Maiorana et al., 2023*). A strike-slip transfer zone developed at this time (the Capo-Granitola Sciacca Fault Zone), which is interpreted by different authors as a wide active lithospheric structure that exhibits left-lateral kinematic movement, crossed the central part of the Sicily Channel (*Argnani et al., 1986; Antonelli et al., 1988*; *Fedorik et al., 2018; Civile et al., 2018; Ferranti et al., 2019; Palano et al., 2020*; Civile et al., 2021) (Fig. 1).

2.2 Seismicity and geodetic data

Historical seismicity in the Sicily Channel is poorly documented and limited to few small magnitude earthquakes (M<4.7) located close to Pantelleria Island (Fig. 2a) while southern

Sicily was the locus of destructive earthquakes such as the 1968 M_w6.4 Belice event (*Guidoboni et al. 2007*). Occurrence of moderate historical earthquakes have been documented also offshore the Sicilian southern coast (1652, 1724, 1727, 1817, 1831). Some of these events (1831, 1891, and 1816-17) were described as related to volcanic activity (*Spampinato et al., 2017* and references therein). Seismic monitoring of the Sicily Channel started in the early 80s when a one-component station was installed on Pantelleria islands (*Spampinato et al., 2017*). Since then, other stations have been installed on Linosa and Lampedusa islands, resulting, however, in a not optimal network geometry, which has also shown discontinuous functioning due to the lack of regular maintenance. Despite these limitations, a set of low-to-moderate earthquakes have been recorded, evidencing tectonic activity in the channel (Fig. 2a) and highlighting two major fault zones, located to the west and east of the GTS, respectively. The first corresponds to the Capo-Granitola Sciacca Fault Zone and runs from Sciacca to Linosa Island in an NNE-SSW direction (Fig. 1) (*Calò and Parisi, 2014; Civile et al., 2018; Fedorick et al., 2018; Ferranti et al., 2019; Civile et al., 2021*). The second is the Scicli-Ragusa Fault System (Fig. 1) extending from southeast Sicily, through Ragusa, to the offshore Sicily Channel. The entire fault zone has shown evidence of left-lateral strike-slip activity (*Catalano et al., 2008*), which is associated with restraining and releasing bends between the various en-echelon segments (*Grasso and Reuther, 1988*). Available focal mechanisms for the Sicily Channel (for events with M_w>4) show prevailing strike-slip features; few events with normal mechanisms have been located south of Malta islands, while events with reverse mechanisms are located in south-eastern Sicily (Fig. 2a).

The geodetic monitoring of the Sicily Channel is currently limited to a few GNSS stations continuously operating since 2001. Estimated GNSS velocities, referred to an Africa-fixed reference frame (Fig. 2b), highlight that LAMP station shows a residual velocity of ∼1 mm/yr towards SSE, evidencing a small deviation with respect to the Africa plate. Stations located on the Hyblean-Malta plateaus are moving toward ENE with rates of ∼2.3 mm/yr, while stations in Pantelleria (PZIN) and on western Sicily move toward E and SE, with rates ranging between ∼3.8 and 2.1 mm/year, respectively. More in detail, the diverging pattern of MALT and LAMP stations shows a significant stretching across the Linosa and Malta Grabens, while the motion of PZIN with respect to MALT and LAMP stations suggests a general contraction of the central sector of the regions. Indeed, geodetic strain-rate estimations (e.g., *Palano et al., 2012; 2020*) highlight that the western sector of the channel is dominated by a prevailing E-W contractional field of ca. 20-30 nanostrain/yr, while the eastern sector is characterized by a strike-slip deformation field (up to 15 nanostrain/yr).

2.3 Volcanic activity

The Sicily Channel is characterized by volcanic activity spanning from historical eruptions to prehistoric and Miocene-age magmatism. Several well-documented eruptions occurred in the last two centuries. In 1831, an eruption at Graham Bank gave rise to the temporary island of Ferdinandea (also known as Foerstner volcano), which emerged about 65 m above sea level (*Washington, 1909; Colantoni et al., 1975; Corti et al., 2006; Conte et al., 2014*). Other eruptions were recorded in 1891 approximately 5 km northwest of Pantelleria (*Washington, 1909*), in 1941 at the Pinne Marine Bank on the southeastern edge of Graham Bank (*Imbò, 1965; Carapezza et al., 1979*), and again in 1981 near Pantelleria Island (*Washington, 1909*).

Prehistoric activity is also evident in the region. Prior to the Last Glacial Maximum (ca. 20 ka B.P.), a tectonic episode along the Capo-Granitola Sciacca Fault Zone produced several volcanic structures (*Lodolo et al., 2019*). Even older magmatism, dating to the late Miocene, has been identified on a submerged seamount east of Nameless Bank (Beccaluva et al., 1981).

In the Graham Bank region, geomorphic features such as pockmarks, mounds, and volcanic seamounts have been recognized, many of which are associated with fluid emissions (*Spatola et al., 2018*). These features exhibit fault-controlled geometries consistent with the Plio-Pleistocene extensional tectonics affecting the northwestern Sicily Channel. Comparable volcano-tectonic relationships are observed in the volcanic seamounts around the Pantelleria Graben, such as the Angelina Seamount (*Civile et al., 2010; Lodolo et al., 2012*).

3. Sicily Channel stratigraphy and Pre-Plio-Quaternary paleogeography

The African continental margin sediment section was incorporated in the Sicilian–Maghrebian fold-and-thrust belt (*Antonelli et al., 1988; Catalano et al., 1996*). These sediment units, dating back to the Late Triassic, include three main carbonate platform successions: Trapanese (Adventure Plateau), Saccense (Sciacca zone), and Iblean (Gela and Iblean offshore) (Figs. 3). From the Late Triassic to the Middle Liassic, shallow platform dolomites and limestones (Sciacca and Inici Fms.) are followed by Toarcian-Eocene pelagic seamount and deep marine limestones and marls (Buccheri, Chiaramonte, Hybla, and Amerillo Fms.) (Figs. 3, 4a-c). In the Iblean domain, extending from the Malta Plateau to the offshore of the Agrigento coast, similar sequences of Late Triassic-Middle Liassic shallow platform and deep marine carbonates and shales (Gela, Noto, Streppenosa, Siracusa, and Modica Fms.) are followed by Toarcian-

Eocene pelagic and deep marine limestones and marls (Buccheri, Chiaramonte, Hybla, and Amerillo Fms.) (Fig. 3), which are capped by external platform carbonates, marls, and evaporitic deposits (Ragusa, Tellaro, and Gessoso-Solfifera Fms.) from the Oligocene-Miocene (Figs. 3, 4d-f). In the Lower Cretaceous, deep-water sedimentation prevailed, represented by the Hybla and Amerillo Fms. (Figs. 3, 4b). This sedimentation continued until the Oligocene, when a shift in sedimentary conditions occurred. In the Iblean zone and Madrepore Bank, shallow-sea carbonate sedimentation (Ragusa Fm.) persisted (Figs. 3, 4c-d), while in the Adventure Plateau zone, clastic sedimentation dominated (*Antonelli et al., 1988*). During the Oligocene-Miocene, the uplift of the western sector of the Sicily Channel reorganized the distribution of emerged lands, forming regional highs like the Mazara-Sciacca high, and giving rise to shallow-water carbonate deposits in the Iblean sector to the east *(Antonelli et al., 1988*). The Messinian event resulted in the deposition of significant evaporitic deposits (Gessoso-Solfifera Fm.) (Fig. 3, 4f). After the Messinian Salinity Crisis, Plio-Quaternary clastic deposits (Trubi and Ribera Fms.) dominate (Fig. 3), marking a rapid return to marine conditions, associated with megafloods (*Micallef et al., 2017*) and the accumulation of contouritic deposits (*Van Dijk et al., 2023*). The sedimentation includes alternating layers of clay, marl, and sand, deposited from shelf areas to deeper pelagic basins within grabens (Fig. 1).

4. Data and methods

An extensive review of the Sicily Channel literature was conducted to extract the Post-Messinian major tectonic and structural features, along with the main regional unconformities, to better constrain the stratigraphic architecture of the area and to refine the timing of activity of the main tectonic structures.

As part of this study, we present line drawings of nine seismic profiles (Lines 1 to 9; locations in Fig. 6), accompanied by their corresponding uninterpreted seismic images (Figs. 7–12). Geological and structural data interpretation is based on seismic profiles already published in the literature (see Tabs. 1, 2 in Suppl. Mat. for seismic line references and details). These seismic lines cover the most representative Sicily Channel sectors (Adventure Plateau, Sciacca offshore, Gela Foredeep Basin, Malta, Linosa, and Pantelleria grabens, respectively) (Fig. 1).

The key horizons, significant for the current review study, were categorized for each sector of the Sicily Channel based on their attributed age and their relevance to the different tectonic phases that occurred in these areas (Tab. 3 in Suppl. Mat.). The line drawings faithfully reproduce the interpretations from the source publications, with no changes to the original structural interpretations (Tab. 1 in Suppl. Mat.)backt

. The only adjustment made was graphical harmonization: consistent color schemes were used to distinguish between Pre-Plio-Quaternary and Plio-Quaternary sequences, as well as to mark the main unconformities.

To support a unified stratigraphic interpretation across the different sectors, a reference stratigraphic framework was developed by correlating stratigraphic markers and unconformities among all the profiles (Fig. 5a, b). This stratigraphic framework was then applied to the various seismic line drawings, enabling the creation of a comparative stratigraphic model (Fig. 5b). This harmonization highlights the similarities and differences among the sectors, helping to clarify the regional tectonic evolution and enabling a coherent stratigraphic chronology for the Sicily Channel.

Following the establishment of the unified framework, the stratigraphic interpretation of each profile was aligned accordingly. Dashed lines were added to indicate unconformities that pass to correlative unconformities or that are likely present but were not explicitly shown in the original publications, and this modification specifically applies to the Plio-Quaternary sequences.

A compilation of the main faults along with their kinematic was extracted from the available literature (see Fig. 13 for the literature considered) and public database, such as INQUA (http://portalesgi.isprambiente.it/it/node/627) and ITACHA (https://sgi.isprambiente.it/ithaca/viewer/index.html), in order to create a summary structural map of the Sicily Channel (Fig. 13). The map was georeferenced with World Geodetic System 84 (WGS84) coordinate reference system on bathymetric data derived from EMODnet (http://www.emodnet-bathymetry.eu/), and different colours were assigned to the structural features coming from different authors/databases to highlight the information source (Fig. 13).

5. Review of Plio-Quaternary structural features in the Sicily Channel

5.1 Adventure Plateau

Situated in the northwest of the Sicily Channel, the 80,000 km^2 Adventure Plateau is the shallowest portion of the Sicily Channel. Water depths are generally just over 150 m (Figs. 1, 2) (*Corti et al., 2006; Civile et al., 2014*). In the Tortonian, contractional deformation—coeval with the opening of the Tyrrhenian Sea and the southward propagation of the Sicilian–Maghrebian fold-and-thrust belt—led to the formation of thrust sheets, where portions of the carbonate substratum were stacked and displaced along ESE-verging thrusts and back-thrusts (*Catalano et al., 2000; Civile et al., 2015*).

During the Messinian, the northern part of the Adventure Plateau was affected by widespread compressional tectonics, and ESE-verging thrusts and back-thrusts were generated, all belonging to the orogenic domain of the ETF representing the lowermost structural level of the Sicilian-Maghrebian Chain (*Lentini et al. 1990, 1994, 1996; Antonelli et al., 1988; Argnani et al., 1986; Civile et al., 2014*). This compressional tectonic is evidenced by the ETF to the NW, and by the ATF to the SE (*Catalano et al., 1985, 1995; Lentini et al., 1990, 1994; Civile et al., 2014; Milia et al., 2021*) (Figs. 7, 13). The activity of the NE-trending Thrust System is associated with the Adventure Foredeep (*Argnani et al. 1986, 1987; Argnani 1993a, b; Civile et al., 2015*): a wide basin filled by clastic sedimentation, affected by shortening processes and partially detaching from its substratum during the Late Messinian (*Argnani 1993a, b; Grasso 2001*).

Lentini et al. (*1990*) suggested that this compressional system is sealed by Plio-Quaternary deposits, but a recent reactivation of the ETF is proposed by *Torelli et al*. (*1993*). *Civile et al*. (*2014*) interpreted the ETF as consisting of several SE-verging thrusts affecting both the Top of Carbonate succession (TCS, ca. 66 - 23 Ma) and the Base of Terravecchia (BTF, ca. 11.6 Ma) horizons (Figs. 7, 13; Tab. 3 in Suppl. Mat.). The BTF horizon appears folded and disrupted, whereas the Top of Miocene (TMS, ca. 5.3 Ma) and the shallowest Plio-Quaternary sediments do not seem to be affected by thrusting (Fig. 7). This shallowest Plio-Quaternary sequence, approximately 0.1 s/TWT thick, is generally undeformed in the seismic profiles (Fig. 7), except for one SE-verging thrust that clearly affects both the Pre- and Post-Messinian successions, including the seabed, providing evidence of recent tectonic reactivation of the ETF (Figs. 7, 13).

5.2 The Capo-Granitola Sciacca Fault Zone

The Adventure plateau is bounded to the East by a wide NS-trending, lithospheric-scale transfer zone located between the ESE verging thrusts of the Adventure plateau and the front of the Sicilian–Maghrebian fold-and-thrust belt (*Argnani et al., 1988; Argnani, 1990; Civile et al., 2008, 2010, 2014; Di Stefano et al., 2015; Palano et al., 2020*). This transfer zone is about 100 km long and extends in the offshore area separating the Pelagic graben to the West from the Malta and Linosa grabens to the East. It is associated with a wide left-lateral active fault zone (Figs. 1, 2a) that is believed to affect the entire continental crust and the upper mantle to a depth of at least 70 km, as suggested by relocated seismicity and geochemical evidence (*Caracausi et al., 2005; Calò and Parisi, 2014*).

This major structural system was interpreted as related to the activity of thrust faults (*Monaco et al*., *1996*) with late Quaternary activity and as the offshore extension of the causative fault of the 1968 Belice earthquake (Fig. 2a). On the other hand, a sequence of thrust sheets in the Sciacca area, involve shallow to deep water carbonates and Tertiary terrigenous and clastic carbonate deposits belonging to the Trapanese and Saccense domains but are sealed by Post-Messinian basinal deposits (*Catalano et al*., *2000*).

A different interpretation is proposed by *Di Stefano et al*. (*2008*) and *Lentini et al*. (*2014*) who suggest that undeformed sequences of the Pelagian block are present in the Sciacca area, in continuity with those outcropping in the Hyblean plateau of southeastern Sicily. *Di Stefano et al*. (*2015*) recognized a segment of the rifted southern passive margin of the Permo-Triassic

Ionian Tethys that runs roughly N-S from San Vito Lo Capo to Sciacca (see location in Fig. 1). They proposed that this inherited paleoceanographic discontinuity may have been reactivated as a major right-lateral strike-slip fault, in response to the horizontal stress field acting in the Central Mediterranean since Late Miocene (*Mantovani et al., 2014*).

More recently, the Sciacca Fault Zone (Fig. 1) has been extensively investigated using seismic reflection profiles and high-resolution morphobathymetric data. *Fedorik et al*. (*2018*) describe the N-S trending transfer zone as bounded by the Capo Granitola Fault to the west and by the Sciacca Fault to the east (Fig. 1), delimiting a 30-km-wide, mostly undeformed basin. The Sciacca Fault was formerly identified by several authors (*Argnani, 1990; Casero and Roure, 1994; Antonelli et al., 1988; Nigro and Renda, 2002; Finetti, 2003; Lentini et al., 2006; Ghisetti et al., 2009*). However, the Capo-Granitola fault to the West does not show clear evidence of present-day tectonic activity, even though it relates to the volcanic area of the Graham Bank to the South (*Fedorik et al., 2018*). The Sciacca Fault is described as a right-lateral tectonic feature that was reactivated in left-lateral during the Pliocene, as testified by the TMS unconformity disruption (*Fedorik et al*., *2018*) (Fig. 7a, b) and present-day focal mechanisms (Fig. 2a). In the northern sector, between the Sicilian coast and the northern margin of the Nerita Bank, the Sciacca Fault seems sealed by Late Pliocene-Quaternary deposits (Fig. 8 a, b). Conversely, the southern segment, located south of Nerita bank, shows clear evidence of active deformation (Fig. 7a).

A different interpretation of the Sciacca fault is provided by *Ghisetti et al*. (*2009*) who suggests that it is a positive flower structure related to a N-S transpressive left-lateral system that bounds the ''Sciacca High'', an emergent salient of the Pelagian-African platform. *Civile et al. (2018)* also included the Sciacca Fault in the broader Capo-Granitola Sciacca Fault Zone, which they interpreted as a Quaternary-active system that developed along a late Miocene structural high (interpreted as a foreland peripheral bulge of the Sicilian–Maghrebian fold-and-thrust belt). Part of the foredeep basin was later inverted along the Capo-Granitola Sciacca Fault Zone and, since the late Pliocene, a kinematic shift from right-lateral to left-lateral strike-slip motion with a compressional component has been proposed (*Fedorik et al., 2018*). On the other hand, *Ferranti et al*. (*2019*) argued that the Capo-Granitola Sciacca Fault Zone has been active in left-lateral transpression since the Late Miocene-Early Pliocene (earlier than in other abovementioned interpretations) when pre-existing Late Tortonian-Early Messinian (Late Miocene) extensional or transtensional basins were inverted.

5.3 Pantelleria Graben

The Pantelleria Graben is a large depression of around 90 km in length and 30 km in width, characterized by linear NW-trending flanks controlled by NE- and SW-dipping steep extensional faults on basin mrgins (Figs. 1, 9a, 13) (*Reuther and Eisbacher, 1985; Civile et al., 2008, 2010*).

The southeastern border of the Pantelleria Graben is crossed by the NE-oriented Line 4 (Figure 6 and Fig. 9), which shows, in the SW part of the line, a structural high capped by a 0.78 s/TWT thick Post-Messinian (Plio-Quaternary) succession (Fig. 9a). In this area, the Top of the Calabrian horizon, i.e., the Unconformity 3 (U3, ca. 0.8 Ma; see Tab. 3 in Suppl. Mat.) divides the less deformed upper Plio-Quaternary section (about 0.25 s/TWT thick), from a lower, more deformed portion (about 0.32 s/TWT thick) of the Post-Messinian succession (Fig. 9a). The thickness of the Post- Messinian (Plio-Quaternary) deposits on the southern edge of the graben (Fig. 9a) suggests that the basin was originally wider than it appears today, and that the succession that makes up the southern edge was later uplifted (*Civile et al*., *2021*).

Extensional faulting in the Pantelleria Graben is associated with moderate folding in the graben's infill and this may be explained as related to buried magmatic intrusion (*Civile et al.*, *2021*) (Fig. 9a). In this zone, several high-angle NE- and SW-dipping and NW-SE-oriented normal faults disrupt the TMS, the U3, as well as the Unconformity 2 (U2, ca. 2.6 - 1.33 Ma; Tab. 3 in Suppl. Mat) and the Unconformity 1 (U1, ca. 4.1 - 3.3 Ma), but these faults are sealed by the shallower Plio-Quaternary sediments (Fig. 9a; Tab. 3 in Suppl. Mat).

The Plio-Quaternary sediment thickness variation across Line 4 (Figure 9) indicates that a positive tectonic inversion, probably related to a transpressive feature, may have occurred along the WNW-oriented, NNE-dipping fault that borders the Pantelleria Graben to the southwest, leading to tectonic uplift (Figs. 9a, 13). The juxtaposition of areas with contrasting tectonic regimes (transpressive versus extensional) supports the hypothesis of a possible NE-trending strike-slip structure acting as a boundary between them (*Civile et al., 2021*). On the other hand, the northern margin of the Pantelleria Graben is marked by a NW-trending structural high, affected by an array of active, high-angle NW and SW-dipping extensional faults (Fig. 13).

5.4 Malta and Linosa Grabens

The Malta Graben is a NW-SE oriented sigmoidal-shaped and more than 160 km long tectonic depression in the central Sicily Channel (Figs. 1, 10a) (*Civile et al., 2021; Maiorana et al., 2023*). A width of about 22 km is observed in the northwestern part of the graben, while in the southern portion it widens up to 30 km (*Civile et al., 2021*). The maximum water depth of about 1700 m is reached in the northwestern part of the graben (Figs. 1, 10a), where the depression is bounded by two prominent seafloor scarps associated with two high-angle, NW-trending extensional faults, as already evidenced in previous works (Fig. 10a) (*Dart et al., 1993; Putz-Perrier and Sanderson, 2010; Civile et al., 2021; Maiorana et al., 2023*).

According to *Civile et al*. (*2021*) and *Maiorana et al*. (*2023*), the graben's margins show evidence of widespread magmatic intrusions (Fig. 10a). The Post-Messinian (Plio-Quaternary) infill is about 1.5 s/TWT (Fig. 10a), and shows three major unconformities (i.e., U1 , U2 , and U3; Tab. 3 in Suppl. Mat.), each recording distinct deformational episodes (Fig. 10a). The Malta Graben records a first Plio-Quaternary extensional phase, highlighted by the syn-rift geometry of the sediment between U1 and U2, followed by a second phase related to the positive inversion of pre-existing extensional structures affecting U2 and U3. A renewed recent extensional regime is highlighted by the presence of normal faults affecting the seabed along basin margins (*Maiorana et al*., *2023*).

The internal geometry of the Malta Graben sediment infill is characterized by a roll-over anticline structure, formed during an extensional phase and subsequently inverted, causing the folding of the deposits above the TMS and deformation of the seafloor of the central Malta Graben (Fig. 10a) (*Maiorana et al., 2023*). In fact, the seafloor highlights positive relief at least ~150 meters (0.1-0.2 s TWT and water velocity of 1500 m/s), affected by a positive inverted fault penetrating both the Pre- and Post-Messinian sediments and cutting the unconformities U2, U1, U3, and TMS (Figs. 10a, 13). This indicates that contractional tectonics recently occurred inside the Malta Graben (*Maiorana et al., 2023*).

Moving to the south, Line 6 shows that the Linosa Graben consists of a 20 km wide depression with a maximum water depth of about 1550 m (Figs. 1, 13) (C*ivile et al., 2021; Maiorana et al., 2023*). The Post-Messinian (Plio-Quaternary) graben sedimentary fill has a maximum thickness of about 2 s/TWT (Fig. 10b) and contains three unconformities (U1 , U2 , and U3) (see Tab. 3

in Suppl. Mat.). Two high-angle extensional faults along the basin margins penetrate the Pre- and Post-Messinian sediment, establishing a staircase pattern, and are associated with seabed scarps on both sides of the graben (Figs. 10b, 13) (C*ivile et al., 2021; Maiorana et al., 2023*). The Plio-Quaternary infill between U1 and U2 exhibits a clear syn-rift geometry, indicating an extensional phase (Fig. 10b). The internal geometry of the Linosa Graben also shows a rollover anticline involving the TMS (Fig. 10b), extending for about 6-7 km with a NW direction (*Civile et al., 2021; Maiorana et al., 2023*). However, a NW-SE striking and SW dipping fault that affects the TMS and the U1 is well imaged inside the graben, but it is sealed by the shallowest Plio-Quaternary sediments (Fig. 10b). *Civile et al.* (*2021*) and *Maiorana et al*. (*2023*) recently interpreted this peculiar structure as a possible positive inverted fault that shortens the rollover anticline, which appears to be sealed by the U2 unconformity. According to *Maiorana et al*. (*2023*) and *Civile et al*. (*2021*), the Post-Messinian sediments lying above the U2 are interpreted as a post-rift succession with a thickness of 0.82 s/TWT thick. This is separated into an upper undeformed part (0.3 s/TWT) and a lower part that is up to 0.48 s/TWT thick. The upper part is marked by sub-parallel reflectors with onlap terminations against the U3, with the latter serving as the boundary between them.

Finally, according to recent findings by *Civile et al*. (*2021*) and *Maiorana et al*. (*2023*), the Linosa Graben exhibits shallow magmatic intrusions concentrated along its margins (Fig. 10b), whose *Maiorana et al*. (*2023*) attribute to the Linosa II volcanic activity (Fig. 2).

5.5 The Gela Thrust System

As the leading edge of the Sicilian-Maghrebian fold-and-thrust belt, the Gela Thrust Front represents the outermost thrust sheet of the GTS (Figs. 1, 8b, 11a, 12a, 13) (*Ogniben 1969;*

Lentini, 1982; Catalano et al., 1996; Ghisetti et al., 2009; Cavallaro et al., 2017). The Gela Thrust Front extends 20-25 km offshore the coast between Sciacca and Gela, facing the Sicily Channel, where it forms a large south-facing arcuate structure (Figs. 1, 13) (*Ogniben, 1969; Catalano, 1987; Argnani, 1989; Grasso et al., 1991; Butler et al., 1992; Lickorish et al., 1999; Catalano et al., 1996; Corti et al., 2006; Ghisetti et al., 2009; Cavallaro et al., 2017; Maiorana et al., 2023*). A foredeep basin, the so called ''Gela Foredeep Basin'', stretches ahead of the Gela Thrust Front as a WNW-ESE-trending, narrow, and weakly deformed elongated depocenter (Figs. 1, 8b, 11a, 12a, 13), filled by 1-1.2 s/TWT thick Post-Messinian (Plio-Quaternary) sediments (Figs. 8b, 11a, 12a).

The GTS resulted from the accretion of foredeep deposits into the thrust sheets combined with internal deformation of the accretionary wedge (*Lickorish et al., 1999*). *Bianchi et al*. (*1989*) describe the GTS as a composite structure, including an upper unit consisting of Oligocene-Serravallian sandstones, Tortonian clays (Terravecchia Fm.), and Messinian-Pliocene units thrusted over a further sequence of Tortonian clays (Fig. 3). The allochthonous nature of the GTS was reported by *Butler et al*. (*1992*) and *Lickorish et al*. (*1999*), who called it ''Gela Nappe''. Based on seismic reflection data and petroleum exploration wells, these authors proposed that the Gela Nappe is constituted by a stratigraphic package that is tectonically emplaced and internally shortened by several minor thrusts, with the basal detachment located on top of the Lower Pliocene Trubi Fm. (U1; Figs. 8b, 11a).
Based on well correlations, *Catalano et al.* (*1996*) and *Cavallaro et al.* (*2017*) indicated that the wedge is composed of imbricated clastic, evaporitic, and carbonate units ranging in age from the Oligocene to Pleistocene, resting above the Pleistocene sediments of the Ribera Fm. of the Gela Foredeep Basin. However, all prior studied pointing that the GTS is a thin-skinned

accretionary wedge dominated by compressive tectonics and characterized by a chaotic internal geometry with discontinuous, folded, and faulted reflections due to shortening processes (Figs. 8b, 11a, 12a).

The GTS stacked units' total thickness is ~2 s/TWT (Figs. 8b, 11a, 12a). Close to the major deformation front, SW-verging thrust sheets form an imbricate fan system, which overthrusts the NE-dipping lower-Upper Pliocene foreland deposits and is sealed by the Plio-Quaternary sediments of the Gela Foredeep Basin (Figs. 8b, 11a, 12a). Along the landward dipping basal detachment, located between 1.6 and 2.4 s/TWT, the overall frontal displacement is more than 5 km at an angle of ~8° (Figs. 8b, 11a, 12a), and truncates the U1 and the sediments below (Figs. 8b, 11a). Moreover, the deformation and displacements of the basal detachment along the NW margin of the Gela foredeep (Figs. 8b and 12a) suggest the existence of inherited normal faults that were reactivated with a reverse cmponent (*Cavallaro et al., 2017; Fedorick et al., 2018*), although *Catalano et al*. (*1996*) do not report evidence of such positive reactivation of previous extensional features (Fig. 11a).

The GTS, cutting and translating the TMS unconformity, is sealed and draped by a sedimentary cover, ranging in thickness from 1.5 to 0.4 s/TWT (Figs. 8b, 11a, 12a) ascribed to the Pliocene by *Lickorish et al*. (*1999*). This sediment cover is folded atop the nappe, indicating ongoing movement and internal shortening of the wedge during the Pliocene. The GTS is onlapped by Post-Messinian (Plio-Quaternary) sediments of the Gela Foredeep Basin (Figs. 8b, 11a, 12a). Internal thrusts involved the the TMS, the U1, and the U2, as interpreted in the Gela Foredeep Basin by *Catalano et al*. (*1993, 1996*) and *Cavallaro et al.* (*2017*) (Figs. 8b, 11a, 12a).

On the top of the GTS, the Zanclean (ca. 5.3 Ma) to Gelasian (ca. 2.6 Ma) strata seem to be gradually folded, forming divergent reflections pattern indicating that the accretionary wedge continued advancing southward and undergoing internal shortening during this period (Fig. 11). Furthermore, as noted by previous authors (*Trincardi and Argnani 1990; Lickorish et al. 1999; Cavallaro et al., 2017*), the GTS's surface slope plunges toward the Gela Foredeep Basin, pointing to gravitational instability of the sediments atop the nappe, expressed by shallow and buried landslide bodies in the Gela Foredeep Basin (Figs. 2, 8b, 12a).

5.6 The Madrepore Bank

The GTS is bounded to the South by the Madrepore Bank (Figs. 1, 12a), a NW–SE fault-controlled monocline about 50 km long and 18 km wide, at a depth ranging from 175 to 750 m bsl (Fig. 1) (*Cavallaro et al., 2017; Maiorana et al., 2023*). It is mainly composed of a Pre-Messinian succession and lacks a Post-Messinian (Plio-Quaternary) cover (Fig. 12a) (*Cavallaro et al., 2017*).

To the south, the Pre-Messinian succession is covered by the middle to upper Miocene silty marls of the Tellaro Fm., followed by the Messinian evaporites and by a thin cover of Zanclean -Piacenzian (ca. 5.3 – 3.6 Ma) sediments. The Pre-Messinian succession mainly consists of carbonates and marls (Ragusa Fm. - Oligocene-Early Miocene), limestones (Amerillo Fm. - Late Cretaceous-Eocene), marls (Hybla Fm. - Early Cretaceous), mudstones (Fadhene and Sidi Kralif Fms. - Early Cretaceous), and marls (Buccheri Fm. - Middle Jurassic) (Figs. 3, 4), according to correlations with the Egeria 1 well log proposed by *Cavallaro et al*. (*2017*).

The structural setting is driven by the re-activation of older NW-SE-trending normal faults (*Antonelli et al., 1988; Corti et al., 2006; Cavallaro et al., 2017*) (Figs. 12a, 13). A set of SW-dipping and NW-SE-striking normal faults (Fig. 12a), affects the whole Post-Messinian succession, disrupting the TCS, the TR (Top of Ragusa fm, Oligo-Miocene), and the TMS horizons, and reaching the seabed. Among these, a major SW-dipping normal fault separates the Madrepore Bank from an adjacent depression known as the Madrepore Graben (*Maiorana et al., 2023*), which is filled of about 0.8 s/TWT of Post-Messinian (Plio-Quaternary) sediments. These sediments seal a NW-SE-oriented normal fault system that also penetrates in the Pre-Messinian succession (Fig. 12a).

6. Discussion

The selected seismic lines reported in this study (Figs. 7-12), integrated with a detailed review of the available literature, allow us to reconstruct the main tectonic evolutionary steps of this foreland area since the Late Miocene (Figs. 14, 15, 16).

6.1 Tectonic evolution of the Sicily Channel from Late Miocene to Quaternary time

The Mediterranean region underwent contractional deformation during the Late Miocene due to the Africa-Eurasia plate convergence (D*ercourt et al., 1986; Dewey et al., 1989*). This resulted in the development of the Calabrian arc (*Minelli and Faccenna, 2010; Polonia et al., 2011, 2012; Maesano et al., 2017; Chizzini et al., 2025*) and the Sicilian–Maghrebian fold-and-thrust belt in the northwest of Sicily (Fig. 14, 17a) (*Antonelli et al., 1988; Civile et al., 2021; Sulli et al., 2021*) (Fig. 17a). Within this regional context, the Sicily Channel corresponded to the foreland area of the convergent system.

In the Late Miocene-Lower Pliocene, the Southern Apennines and Ionian slabs retreated rapidly (*Faccenna et al., 2001; Civile et al., 2021; Joliviet et al., 2021*). A sudden reorientation of the stress field and a change in the boundary conditions across the Central Mediterranean.

In this context, Sicily and the Sicily Channel became a transitional area between the slow relative NW movement of the African plate and the eastward opening of the Tyrrhenian Sea (*Civile et al., 2021*). This differential motion was accommodated along the Sicily Channel through different processes: i) the opening of the Pantelleria, Linosa, and Malta Grabens, resulted from a NW-SE-oriented extension of the African plate's foreland area (*Corti et al., 2006; Catalano et al., 2009; Civile et al., 2010; 2021; Maiorana et al., 2023*), possibly with a dextral strike-slip component (*Catalano et al., 2009; Civile et al., 2021*); and ii) the development of two roughly NS-trending regional-scale shear zones: the Capo-Granitola Sciacca Fault Zone in the northewest, activated since the Late Miocene (*Ferranti et al., 201*9) or Lower Pliocene (*Fedorik et al., 2018; Civile et al., 2021*), and the Scicli-Ragusa Fault System in the northeast, mainly onshore but extending offshore toward Malta Island for at least 40 km (*Gardiner et al., 1995; Pellegrino et al., 2016*) (Fig. 14, 17b). Both fault systems are the result of the reactivation in a strike-slip stress regime of previous N-S-oriented Mesozoic paleoceanographic or structural discontinuities, such as extensional faults controlling the platform-to-basin or shallow-to-deeper carbonate platform transitions (*Antonelli et al., 1988; Pellegrino et al., 2016*) (see, for instance, the paleogeographic map in Fig. 4d). In addition, NW-SE and NE-SW-oriented extensional faults also developed nearby Malta Island and the Scicli-Ragusa Fault System (*Antonelli et al., 1988; Gardiner et al., 1995*) (Fig. 14).

During the Lower Pliocene, the Sicilian–Maghrebian fold-and-thrust belt was segmented by the Capo-Granitola Sciacca Fault Zone, resulting in two opposing and verging fold-and-thrust belts: the SE-verging ETF and the South-verging GTS, along with the Gela Thrust Front as the outermost thrust sheet of the latter (*Argnani et al., 1986; Civile et al., 2014; Morticelli et al., 2015*) (Fig. 14). These belts were both marked by vigorous compressional tectonics, evidenced by the presence of thrusts and back-thrusts (*Civile et al., 2021*) (Fig. 14, 17b). Moreover, the

GTS advance induced positive tectonic inversion in the Madrepore Graben, in agreement with the first stage of advancement of the GTS, dated to the Piacenzian (3.13 Ma) as reported by *Cavallaro et al*. (*2017*), *Civile et al*. (*2021*), and *Maiorana et al*. (*2023*).

During the Early Pleistocene (Figure 15), subduction in the Southern Apennines was inhibited by the entrance of the continental Apulian lithosphere at the trench, enhancing the the rapid southeastward migration of the Calabrian Arc (*Filice and Seeber, 2019; Civile et al., 2021*). The ongoing south-southwestward advancement of the GTS transmitted compressive stress to the Sicilian foreland, inducing the positive reactivation of pre-exisiting SE-dipping extensional faults in the Linosa and Malta grabens (*Cavallaro et al., 2017; Civile et al., 2021; Maiorana et al., 2023*) (Fig. 15, 17c). This marks the last stage of the GTS advancement, dated 0.8 Ma (upper Calabrian-U3) (*Di Stefano et al., 1993; Cavallaro et al., 2017; Maiorana et al., 2023*), while the ATF stopped (Fig. 15) (*Argnani et al., 1993a ,b, 1996*).

Simultaneously, compression persisted in the NW sector of the Sicily Channel, and the ETF maintained its southwestward progression; however, thrusts and backthrust active in the Late Miocene-Early Pliocene stopped and were sealed by Plio-Quaternary deposits (*Argnani et al., 1986; Catalano et al., 2000; Civile et al., 2014*) (Fig. 15). Extensional tectonics related to the Malta, Linosa, and Pantelleria Grabens remained active (*Antonelli et al., 1988; Civile et al., 2010; Cavallaro et al., 2017; Civile et al., 2021; Maiorana et al., 2023*), as did NW–SE and NE–SW oriented extensional fault system in the easternmost Sicily Channel, between Malta Island and the Scicli-Ragusa Fault System (*Antonelli et al., 1988; Gardiner et al; 1*995) (Fig. 15).

Strike-slip faults remained active along the Capo-Granitola Sciacca fault zone and the Scicli–Ragusa Fault System, which, combined with the GTS compressive system, were probably partly responsible for the positive inversion observed in Malta, Linosa, and Pantelleria grabens

(Fig. 15, 17c). Throughout the Capo-Granitola Sciacca Fault Zone, transpressional tectonics was active, and the Scicli-Ragusa Fault System may have shifted from a right-lateral to a left-lateral strike-slip motion sense, as a result from a change in the relative direction of motion of the African plate with respect to Eurasia, from NW to NE (*Mantovani et al., 2014*; *Fedorik et al., 2017; Ferranti et al., 2019; Civile et al., 2021*). However, shortening within the GTS ceased around the end of the Early Pleistocene, when the GTS reached its present-day position (*Catalano et al., 1996, 2013; Civile et al., 2021; Maiorana et al., 2023*); in contrast, shortening related to ETF persisted (*Civile et al., 2014*) (Fig. 15).

At present day, Malta and Linosa Grabens show signs of positive inversion of former extensional faults (Fig. 16, 17d). These are primarily two NW-SE oriented, SW-dipping positive inverted faults likely reflecting a response to tectonic plate reorganization and a possible subduction polarity reversal (*Sulli et al., 2021; Maiorana et al., 2023*). The associated stress field promotes the localized reactivation of these pre-existing extensional structures, which represent inherited weak zones (*Sulli, 2000; Maiorana et al., 2023*). This last stage is also accommodated by the ongoing activity of the Capo-Granitola Sciacca Fault Zone (Fig. 16, 17d), which is tectonically active, as testified by the occurrence of seismic events depicting a roughly N-S arrangement with focal mechanisms characterized by strike-slip kinematics (Fig. 2a).

The available GNSS data, collected in the last two decades (Fig. 2b), show a diverging pattern between MALT and LAMP stations, suggesting a stretching across the Linosa and Malta grabens. This could represent the incipient reactivation of extensional faults, as evidenced by available normal faulting focal mechanisms though this activity has not yet produced observable deformation in the sedimentary cover (Fig. 2a). Also, the ETF remains active, as suggested by seafloor deformation described by *Torelli et al.* (*1993, 1995*) and *Civile et al*.

(*2014*) (Fig. 16). In the eastern sector, particularly the Malta Plateau, recent normal faulting has generated a series of seafloor horst blocks (*Antonelli et al., 1988; Gardiner et al., 1995*) (Fig. 16).

6.2 Plio-Quaternary structures in the Sicily Channel and implications for foreland (unstable) tectonics

Seismic reflection profiles indicat widespread evidence of Plio-Quaternary tectonic activity in the Sicily Channel foreland, despite it should be part of a relatively stable area. According to the structural map in Fig. 14, the Sicily Channel hosts three major coexisting tectonic regimes.

The southernmost portion of the area is site of extensional tectonics, exemplified by a set of NW-SE-striking normal faults, located at approximately 170 km from the orogen fronts to the north (ETF and GTS). This extensional regime is responsible for the development of Pantelleria, Linosa, and Malta grabens (Fig. 12), as well as for the development of the roughly N-S trending volcanic belt that stretches from Lampedusa to the Adventure Plateau (*Lodolo et al., 2019*) (Fig. 2b).

A recent compressional tectonic regime is responsible for folding and shortening processes within the grabens as evidenced by NW-SE-oriented high-angle reverse faults, due to inversion of Mesozoic normal faults (C*avallaro et al., 2017; Civile et al., 2021; Maiorana et al., 2023*). However, extensional focal mechanisms of recent earthquakes combined with current increasing distance between LAMP and MALT stations (Fig. 2 a,b) suggest active NE-SW stretching in the grabens (Fig. 15). Simultaneously, the strike-slip/transpressional regime of the Capo-Granitola Sciacca Fault Zone disrupts the NW-SE extensional faults connected to Malta, Linosa, and southern termination Pantelleria grabens. This results in the overlap of the two distinct tectonic regimes: strike slip/transpressive on one side and extension within the garbens (Fig. 12).

All of the tectonic structures related to the extensional and transpressive tectonic regimes affect the Pre-Pliocene layers down to the basement, thus suggesting thick-skinned tectonics in the Sicily Channel (*Cavallaro et al., 2017; Civile et al., 2021; Maiorana et al., 2023*). The deep seated features inverted faults appear to be strongly influenced by the geometry and orientation of the structures developed during the previous phase of extension (*Nalpas et al., 1995; Ziegler et al., 1995; Amilibia et al., 2005; Del Ben et al., 2010; Rodríguez-Salgado et al., 2022*). Reactivation of extensional faults often occurs as reversal when the pre-existing extensional fabric is almost orthogonal to the direction of shortening (*Ziegler et al., 1995*; *Cooper and Warren, 2015*; *Rodríguez-Salgado et al., 2022*). In the Sicily Channel, the stress field associated with the post Middle-Pleistocene inversion (C*avallaro et al., 2017; Civile et al., 2021; Maiorana et al., 2023*) is almost orthogonal to the NW-SE-striking extensional faults. As a result, these faults were reactivated in a compressive regime even though they are far form the compressional systems.

There are several cases in the Mediterranean area where compressional stresses were transmitted far from the main deformation fronts, inducing the inversion of rifted and/or flexed foreland basins. Among them, the northern Tunisia, that shows a widespread compressional Eocene event associated with tectonic inversion of several normal faults (*Masrouhi et al., 2008; Khomsi et al., 2009*; *Rigane et al., 2011*). In the Adriatic Sea, the main phase of emplacement of the outer Apennine chain is associated with the reactivation of Mesozoic extensional faults as reverse faults (*Calamita et al., 1991; Scisciani, 2009; Satolli and Calamita, 2012; Pace et al., 2015*). Finally, several positive inverted faults activated by the advance of the Calabrian Arc and Hellenic fold-and-thrust belt are described in the southern Adria Plate in the Ionian Sea (*Del Ben, 2009; Del Ben et al., 2010; Basso et al., 2021; Chizzini et al., 2022, 2023*).

It is important to point out that the presence of fluid-related features, well documented in the Sicily Channel in the form of pipes, bright spots, mud volcanoes, zones of acoustic blanking, and active seepage (*Spatola et al., 2018; Civile et al., 2023; Maiorana et al., 2024*), may play an important role in driving tectonic activity since they can reduce the friction along the fault planes (*Sibson, 1995*). Morover, the intrusion of magmas and the consequent high heat flow can further enhance intra-plate deformation in this area. The lithosphere of a rift system that characterized by increased heat flow and magma production is not as strong as that of thermally stable rift zones (*Ziegler et al., 1995; Rooney, 2017; Shillington, 2020; Pérez-Gussinyé et al., 2023*). The existence of volcanic zones (Fig. 2), magmatic intrusions, and associated fluids in the Sicily Channel (Figs. 7, 8) are linked to a shallow Moho (17–18 km in the Malta and Linosa grabens) (*Maiorana et al., 2023; Bongiovanni et al., 2025*), and this may have contributed to weakening the region and making it prone to tectonic deformation with a high variability of tectonic regimes.

In the Sicily Channel, the interplay between slab-pull and roll-back, as plate driving forces, are considered the main processes triggering the extensional tectonics that affected this area (*Argnani, 1990; Govers and Wortel, 2005; Rosenbaum et al., 2008; Argnani, 2009; Arab et al., 2020; Maiorana et al., 2023*). In this scenario, the slow and oblique convergence along the irregular Africa-Eurasia plate boundary (*Bellon and Letouzey, 1977 ; Dercourt et al., 1986; Dewey et al., 1989; Stampfli and Borel, 2004; Mascle and Chaumillon, 1997; Polonia et al.,* *2011; Jolivet et al., 2021*) appears to be the main mechanism driving plate-boundary reorganization and structural development in this area.

7. Conclusions

Based on a detailed review of the available structural and stratigraphic data, we provide a general overview of the main tectonic features affecting the Sicily Channel region and its post Miocene tectonic evolution that shows a strict interplay between deep and shallow processes even far away from the boundary between the converging plates.

1) The forelans area of the Sicily Channel is shaped by the interaction of multiple tectonic processes linked to the complex geodynamic evolution of the Central Mediterranean driven by plate convergence, slab rollback and different rates of collision along the plate boundary.
2) Inherited structural discontinuities and preexisting extensional faults, were reactivated in a compressional regime since they correspond to zones of preferential strain concentration that accommodate intra-plate shortening, even if these zones are located far from the orogens.
3) The relationship between pre-existing structural grain, the stress orientation, and the occurrence of circulating fluids play an important role in the localization of present-day tectonic structures as well as on the future basin architecture.
4) The structural evolution of the Sicily Channel and its geodynamic setting suggest that foreland regions can represent areas of intense tectonic deformation and can be subject to a multi—phase tectonic evolution even-though they are far form the plate boundaries.

This new compilation of structural maps of the Sicily Channel is of interest for anyone working on geohazards of this complex region and relating seismic events to active structures, as well as for interpreting and better constraining the kinematics of this area and other foreland locations worldwide.

Acknowledgment

This work was funded by the University of Parma – Fondazione Cariparma 2020. We gratefully acknowledge OGS (Istituto Nazionale di Oceanografia e di Geofisica Sperimentale, Trieste) and E. Lodolo for granting access to the MS and PANT seismic databases and for permission to publish seismic images. We also thank Editor Laurent Jolivet and two anonymous reviewers for their constructive comments, which significantly improved the quality of this work.

References

Adam J, Reuther CD, Grasso M, Torelli L. 2000. Active fault kinematics and crustal stresses along the Ionian margin of southeastern Sicily. Tectonophysics 326(3-4): 217–239.

Aksu AE, Hall J, Calon TJ, Barnes MC, Güneş P, Cranshaw JC. 2018. Messinian evaporites across the Anaximander mountains, Sırrı Erinç Plateau and the Rhodes and Finike basins, eastern Mediterranean Sea. Marine Geology 395: 48–64. https://doi.org/10.1016/j.margeo.2017.09.013

Allen PA, Homewood P, eds. 2009. Foreland basins. John Wiley & Sons.

Allen PA, Allen JR. 1990. Basin Analysis, Principles & Application. Blackwell Scientific Publication, pp. 115–126.

Amilibia Cabeza A, McClay KR, Sābat i Montserrat F, Muṇoz JA, Roca i Abella E. 2005. Analogue modelling of inverted oblique rift systems. Geologica Acta 3(3): 251–271.

Antonelli C. 1989. A failure-inducement model of research and development expenditure: Italian evidence from the early 1980s. Journal of Economic Behavior & Organization 12(2): 159–180.

Antonelli M, Franciosi R, Querci A, Ronco G, Vezzanin F. 1988. Paleogeographic evolution and structural setting of the northern side of the Sicily Channel. In: Società Geologica Italiana, 74. Congresso Nazionale, Relazioni, pp. 79–86.

Arab M, Maherssi C, Granjeon D, Roure F, Dverchere J, Cuilhe L, Hassaim M, Mouchot N, Doublet S, Khomi S. 2020. On the origin and consequences of crustal-scale extension between Africa and Sicily since Late Miocene: insights from the Kaboudia area, western Pelagian Sea. Tectonophysics 795: 228565.

Argnani A. 1993a. Neogene tectonics of the Strait of Sicily. In: Max MD, Colantoni P, eds. Geological development of the Sicilian-Tunisian Platform. UNESCO Report in Marine Science 58: 55–60.

Argnani A. 1993b. Neogene basins in the Strait of Sicily (Central Mediterranean): tectonic settings and geodynamic implications. In: Boschi E et al., eds. Recent evolution and seismicity of the Mediterranean region. Kluwer Academic Publication, Dordrecht, pp. 173–187.

Argnani A, Bonazzi C. 2005. Malta Escarpment fault zone offshore eastern Sicily: Pliocene-Quaternary tectonic evolution based on new multichannel seismic data. Tectonics 24(4).

Argnani A. 1990. The Strait of Sicily rift zone: foreland deformation related to the evolution of a back-arc basin. Journal of Geodynamics 12(2-4): 311–331.

Argnani A. 2018. Subduction evolution of the Dinarides and the Cretaceous orogeny in the Eastern Alps: Hints from a new paleotectonic interpretation. Tectonics 37(2): 621–635.

Argnani A, Cornini S, Torelli L, Zitellini N. 1986. Neogene-Quaternary foredeep system in the Strait of Sicily. Mem. Soc. Geol. It. 36: 123–130.

Basso J, Artoni A, Torelli L, Polonia A, Carlini M, Gasperini L, Mussoni P. 2021. Oblique plate collision and orogenic translation of the Southern Apennines revealed by post-Messinian interregional unconformities in the Bradano Basin (Ionian Sea - Central Mediterranean). Marine and Petroleum Geology 128: 104999. https://doi.org/10.1016/j.marpetgeo.2021.104999

Beccaluva L, Colantoni P, Di Girolamo P, Savelli C. 1981. Upper submarine volcanism in the Strait of Sicily (Banco Senza Nome). Bulletin of Volcanology 44: 573–581.

Basilone, L., 2009. Mesozoic tectono-sedimentary evolution of Rocca Busambra in western Sicily. Facies. 55, 115–135. https://doi.org/10.1007/s10347-008-0156-2.

Bellon H, Letouzey J. 1977. Volcanism related to plate tectonics in the western and eastern Mediterranean. In: Structural History of the Mediterranean Basins. Paris: Technip, pp. 165–184.

Del Ben A, Geletti R, Mocnik ARIANNA. 2010. Relation between recent tectonics and Mesozoic inherited structures of the central-southern Adria plate. Bollettino di Geofisica Teorica e Applicata 51(2-3): 99–115.

Boccaletti M, Cello G, Tortorici L. 1987. Transtensional tectonics in the Sicily Channel. Journal of Structural Geology 9(7): 869–876.

Bongiovanni, S., Maiorana, M., D'Alessandro, A., Martorana, R., Sulli, A., 2025. Lithospheric features revealed by a new Moho map in the central-western Sicily Channel. Sci. Rep. 15, 1–15. https://doi.org/10.1038/s41598-025-01189-7

Burollet PF, J. Mugniot JM, and Sweeney P. 1978. The geology of the Pelagian block: the margins and basins of southern Tunisia and Tripolitania, in The Ocean Basins and Margins: The Western Mediterranean. Vol. 4b, A. E. M. Nairn, W. H. Kanes, and F. G. Stelhi, Eds., pp. 331–359, Plenum, New York.

Butler RW. 2009. Relationships between the Apennine thrust belt, foredeep and foreland revealed by marine seismic data, offshore Calabria. Italian Journal of Geosciences 128(2): 269–278. https://doi.org/10.3301/IJG.2009.128.2.269

Butler RW, Lickorish WH, Grasso M, Pedley HM, Ramberti L. 1995. Tectonics and sequence stratigraphy in Messinian basins, Sicily: constraints on the initiation and termination of the Mediterranean salinity crisis. Geological Society of America Bulletin 107(4): 425–439.

Butler RWH, Grasso M, La Manna F. 1992. Origin and deformation of the Neogene-Recent Maghrebian foredeep at the Gela Nappe, SE Sicily. Journal of the Geological Society 149(4): 547–556. https://doi.org/10.1144/gsjgs.149.4.0547

Calamita F, Deiana G, Invernizzi MC, Pizzi A. 1991. Tettonica. In: L'AMBIENTE FISICO DELLE MARCHE, pp. 69-80. SELCA.

Calamita F, Satolli S, Turtu A. 2012. Analysis of thrust shear zones in curve-shaped belts: Deformation mode and timing of the Olevano-Antrodoco-Sibillini thrust (Central/Northern Apennines of Italy). Journal of Structural Geology 44: 179–187.

Calanchi N, Colantoni P, Rossi PL, Saitta M, Serri G. 1989. The Strait of Sicily continental rift systems: physiography and petrochemistry of the submarine volcanic centres. Marine Geology 87: 55–83. https://doi.org/10.1016/0025-3227(89)90145-X.

Calò M, Parisi L. 2014. Evidences of a lithospheric fault zone in the Sicily Channel continental rift (southern Italy) from instrumental seismicity data. Geophysical Journal International 199(1): 219–225. https://doi.org/10.1093/gji/ggu249

Camerlenghi A, Del Ben A, Hübscher C, Forlin E, Geletti R, Brancatelli G, Micallef A, Saule M, Facchin L. 2020. Seismic markers of the Messinian salinity crisis in the deep Ionian Basin. Basin Research 32(4): 716–738.

Carapezza M, Nuccio PM, Valenza M. 1981. Genesis and evolution of the fumaroles of Vulcano (Aeolian Islands, Italy): a geochemical model. Bulletin Volcanologique 44: 547–563.

Carminati E, Doglioni C. 2012. Alps vs. Apennines: The paradigm of a tectonically asymmetric Earth. Earth-Science Reviews 112(1-2): 67–96. https://doi.org/10.1016/j.earscirev.2012.02.004.

Carminati E, Lustrino M, Cuffaro M, Doglioni C. 2010. Tectonics, magmatism and geodynamics of Italy: what we know and what we imagine. Journal of the Virtual Explorer 36: 10-3809.

Casero, P., Cita, M.B., Croce, M., De Micheli, A., 1984. Tentativo di interpretazione evolutiva della scarpata di Malta basata su dati geologici e geofisici. Mem. Soc. Geol. It. 27, 235–253.

Catalano, R., D'Argenio, B., 1982. Schema geologico della Sicilia. In: Catalano, R., D'Argenio, B. (Eds.), Guida alla geologia della Sicilia occidentale. —Soc. Geol. It., Palermo

Catalano R, Franchino A, Merlini S, Sulli A. 2000. Central western Sicily structural setting interpreted from seismic reflection profiles. Mem. Soc. Geol. It. 55: 5–16.

Catalano R, Infuso S, Sulli A. 1995. Tectonic history of the submerged Maghrebian Chain from the Southern Tyrrhenian Sea to the Pelagian Foreland. Terra Nova 7(2): 179–188.

Catalano R, Valenti V, Albanese C, Accaino F, Sulli A, Tinivella U, Gasparo Morticelli M, Zanolla C, Giustiniani M. 2013. Sicily's fold–thrust belt and slab roll-back: the SI. RI. PRO. seismic crustal transect. J. Geol. Soc. 170(3): 451–464.

Catalano S, De Guidi G, Lanzafame G, Monaco C, Tortorici L. 2009. Late Quaternary deformation on the island of Pantelleria: new constraints for the recent tectonic evolution of the Sicily Channel Rift (southern Italy). J. Geodyn. 48(2): 75–82.

Catalano S, De Guidi G, Monaco C, Tortorici G, Tortorici L. 2008. Active faulting and seismicity along the Siculo–Calabrian Rift Zone (southern Italy). Tectonophysics 453(1-4): 177–192. https://doi.org/10.1016/j.tecto.2007.05.008

Catalano S, De Guidi G, Lanzafame G, Monaco C, Tortorici L. 2009. Late Quaternary deformation on the island of Pantelleria: new constraints for the recent tectonic evolution of the Sicily Channel Rift (southern Italy). Journal of Geodynamics 48(2): 75-82.

Cavallaro D, Brancolini G, Lodolo E, Forlin E, Accaino F, Zecchin M, Brancatelli G. 2021. Morphostructural Setting and Tectonic Evolution of the Central Part of the Sicilian Channel (Central Mediterranean). Lithosphere 2021(1): 1–24. https://doi.org/10.2113/2021/7866771

Cavallaro D, Monaco C, Polonia A, Sulli A, Di Stefano A. 2017. Evidence of positive tectonic inversion in the north-central sector of the Sicily Channel (Central Mediterranean). Nat. Hazards 86(Suppl. 2): 233–251. https://doi.org/10.1007/s11069-016-2515-6

Cello G. 1987. Structure and deformation processes in the Strait of Sicily "rift zone." Tectonophysics 141(1-3): 237–247. https://doi.org/10.1016/0040-1951(87)90188-0

Chaumillon E, Mascle J. 1997. From foreland to forearc domains: new multichannel seismic reflection survey of the Mediterranean Ridge accretionary complex (Eastern Mediterranean). Marine Geol. 138(3-4): 237–259.

Chizzini N, Artoni A, Torelli L, Basso J, Polonia A, Gasperini L. 2022. Tectono-stratigraphic evolution of the offshore Apulian Swell, a continental sliver between two converging orogens (Northern Ionian Sea, Central Mediterranean). Tectonophysics 839: 229544. https://doi.org/10.1016/j.tecto.2022.229544

Chizzini N, Artoni A, Torelli L, Maiorana M, Sulli A. 2023. Evidence of new diapiric structures in the southern Adria Plate (Eastern Margin of Tethyan Ocean): Implications for Triassic paleogeography and evaporites remobilization during subduction/collision (Northern Ionian Sea, Central Mediterranean). Marine Geology 465: 107162. https://doi.org/10.1016/j.margeo.2023.107162

Chizzini, N., Artoni, A., Torelli, L., Polonia, A., Qadir, A., Gasperini, L., 2025. Accretionary wedge collision in the Ionian Sea: Timing and movement of the Calabrian arc and the Mediterranean ridge in the central Mediterranean Sea. Gondwana Res. 144, 212–238. https://doi.org/10.1016/j.gr.2025.04.011

Civetta L, D'Antonio M, Orsi G, Tilton G.R. 1998. The geochemistry of volcanic rocks from Pantelleria Island, Sicily Channel: petrogenesis and characteristics of the mantle source region. J. Petrology 39(8): 1453–1491. https://doi.org/10.1093/petroj/39.8.1453

Civile D, Baradello L, Accaino F, Zecchin M, Lodolo E, Ferrante G.M, Markezic N, Volpi V, Burca M. 2023. Fluid-Related Features in the Offshore Sector of the Sciacca Geothermal Field (SW Sicily): The Role of the Lithospheric Sciacca Fault System. Geosciences 13(8): 231. https://doi.org/10.3390/jmse12071142.

Civile D, Brancolini G, Lodolo E, Forlin E, Accaino F, Zecchin M, Brancatelli G, Billi A. 2021. Morphostructural setting and tectonic evolution of the central part of the Sicilian Channel (Central Mediterranean). Lithosphere.2021(1). https://doi.org/10.2113/2021/7866771.

Civile D, Lodolo E, Accaino F, Geletti R, Schiattarella M, Giustiniani M, Fedorik J, Zecchin M, Zampa L 2018. Capo Granitola-Sciacca fault zone (Sicilian Channel, Central Mediterranean): structure vs magmatism. Marine and Petroleum Geol. 96: 627–644. https://doi.org/10.1016/j.marpetgeo.2018.05.016

Civile D, Lodolo E, Accettella D, Geletti R, Ben-Avraham Z, Deponte M, Facchin L, Ramella R, Romeo R. 2010. The Pantelleria graben (Sicily Channel, Central Mediterranean): an example of intraplate 'passive' rift. Tectonophysics 490(3-4): 173-183.

Civile D, Lodolo E, Alp H, Ben-Avraham Z, Cova A, Baradello L, Accettella D, Burca M, Centonze J. 2014. Seismic stratigraphy and structural setting of the Adventure Plateau (Sicily Channel). Marine Geophysical Research 35(1): 37–53. https://doi.org/10.1007/s11001-013-9205-5

Civile D, Lodolo E, Zecchin M, Ben-Avraham Z, Baradello L, Accettella D, Cova A, Caffau M. 2015. The lost Adventure Archipelago (Sicilian Channel, Mediterranean Sea): Morpho-bathymetry and Late Quaternary palaeogeographic evolution. Global and Planetary Change 125: 36–47.

Civile D, Lodolo E, Tortorici L, Lanzafame G, Brancolini G. 2008. Relationships between magmatism and tectonics in a continental rift: The Pantelleria Island region (Sicily Channel, Italy). Marine Geol. 251(1–2): 32–46. https://doi.org/10.1016/j.margeo.2008.01.009

Cloetingh S, Eldholm O, Larsen B.T., Gabrielsen R.H, Sassi W. 1994. Dynamics of extensional basin formation and inversion: introduction. Tectonophysics 240(1-4): 1–9.

Cloetingh S, Ziegler P.A., Beekman F, Burov E.B., Garcia-Castellanos D, Matenco L. 2015. Tectonic Models for the Evolution of Sedimentary Basins. In: Treatise on Geophysics: Second Edition, Vol. 6. Elsevier B.V. https://doi.org/10.1016/B978-0-444-53802-4.00117-2

Cogan J, Rigo L, Grasso M, Lerche I. 1989. Flexural tectonics of southeastern Sicily. J. Geodyn. 11(3): 189–241. https://doi.org/10.1016/0264-3707(89)90007-0

Coltelli M, Cavallaro D, D'Anna G, D'Alessandro A, Grassa F, Mangano G, Patanè D, Gresta S. 2016. Exploring the submarine Graham Bank in the Sicily Channel. Ann. Geophys.

Corti G, Cuffaro M, Doglioni C, Innocenti F, Manetti P. 2006. Coexisting geodynamic processes in the Sicily Channel. Spec. Pap. Geol. Soc. Am. 409(05): 83–96. https://doi.org/10.1130/2006.2409(05).

Conte A.M, Martorelli E, Calarco M, Sposato A, Perinelli C, Coltelli M, Chiocci F.L. The 1891 submarine eruption offshore Pantelleria Island (Sicily Channel, Italy): Identification of the vent and characterization of products and eruptive style. Geochemistry, Geophysics, Geosystems. 2014 Jun;15(6):2555-74.

Critelli, S., Martín-Martín, M., 2024. History of western Tethys Ocean and the birth of the circum-Mediterranean orogeny as reflected by source-to-sink relations. Int. Geol. Rev., v. 66 (2), p. 505-515. 10.1080/00206814.2023.2280787

De Alteriis G. 1995. Different foreland basins in Italy: examples from the central and western Adriatic Sea. Tectonophysics 252: 349–373.

DeCelles P.G, Giles K.A. 1996. Foreland basin systems. Basin Research 8(2): 105–123. https://doi.org/10.1046/j.1365-2117.1996.01491.x

DeCelles PG. 2012. Foreland basin systems revisited: variations in response to tectonic settings. In: Busby C, Pérez A.A. (Eds.), Tectonics of Sedimentary Basins: Recent Advances. Blackwell Publishing Ltd., Chichester, UK, pp. 405–426. https://doi.org/10.1002/9781444347166.ch20

Del Ben A. 2009. Earthquakes and Shallow Structures in South Adria: Evidence of Recent Inversion Tectonics. Nova Science Publishers, Inc, pp. 147–163 (Chapter 6).

Del Ben, Geletti R, Mocnik AR. 2010. Relation between recent tectonics and Mesozoic inherited structures of the central-southern Adria plate. Bollettino di Geofisica Teorica e Applicata 51(2-3):99-115.

Dewey JF, Helman ML, Knott SD, Turco E, Hutton DHW. 1989. Kinematics of the western Mediterranean. Geol Soc Lond Spec Publ 45(1): 265–283.

Di Stefano E, Infuso S, Scarantino S. 1993. Plio-Pleistocene sequence stratigraphy of southwestern offshore Sicily from well logs and seismic sections in a high-resolution calcareous plankton biostratigraphic framework. In: Max MD, Colantoni P, eds. Geological Development of the Sicilian-Tunisian Platform. UNESCO Rep Mar Sci 58: 105–110.

Dercourt JE, Zonenshain LP, Ricou LE, Kazmin VG, Le Pichon X, Knipper AL, Grandjacquet C, Sbortshikov IM, Geyssant J, Lepvrier C, Pechersky DH. 1986. Geological evolution of the Tethys belt from the Atlantic to the Pamirs since the Lias. Tectonophysics 123(1-4): 241–315.

Doglioni C, Harabaglia P, Merlini S, Mongelli F, Peccerillo AT, Piromallo C. 1999. Orogens and slabs vs. their direction of subduction. Earth-Science Reviews 45(3-4): 167–208.

Ekström, G., M. Nettles, and A. M. Dziewonski, The global CMT project 2004-2010: Centroid-moment tensors for 13,017 earthquakes, Phys. Earth Planet. Inter., 200-201, 1-9, 2012. doi:10.1016/j.pepi.2012.04.002.

Faccenna C, Funiciello F, Giardini D, Lucente P. 2001a. History of subduction and back-arc extension in the Central Mediterranean. Geophys. J. Int. 145: 809–820.

Faccenna C, Funiciello F, Giardini D, Lucente P. 2001b. Episodic back-arc extension during restricted mantle convection in the Central Mediterranean. Earth Planet. Sci. Lett. 187: 105–116.

Fedorik J, Toscani G, Lodolo E, Civile D, Bonini L, Seno S. 2018. Structural analysis and Miocene-to-Present tectonic evolution of a lithospheric-scale, transcurrent lineament: The Sciacca Fault (Sicilian Channel, Central Mediterranean Sea). Tectonophysics 722: 342–355.

Ferranti L, Pace B, Valentini A, Montagna P, Pons-Branchu E, Tisnérat-Laborde N, Maschio L. 2019. Speleoseismological constraints on ground shaking threshold and seismogenic sources in the Pollino range (Calabria, southern Italy). J. Geophys. Res.: Solid Earth 124(5): 5192–5216.

Ferranti L, Pepe F, Barreca G, Meccariello M, Monaco C. 2019. Multi-temporal tectonic evolution of Capo Granitola and Sciacca foreland transcurrent faults (Sicily Channel). Tectonophysics 765: 187–204. https://doi.org/10.1016/j.tecto.2019.05.002.

Filice, F., Seeber, L., 2019. The culmination of an Oblique Time-Transgressive Aarc Continent Collision: the Pollino Massif between Calabria and the Southern Apennines, Ital. Tectonics 38, 3261–3280. https://doi.org/10.1029/2017TC004932.

Finetti I.R, Del Ben A. 2005. Crustal tectono-stratigraphic setting of the Adriatic Sea from new CROP seismic data. CROP project: Deep seismic exploration of the Central Mediterranean and Italy 1: 519–548.

Finetti I.R. 1984. Geophysical study of the Sicily Channel Rift Zone. Boll. Geofis. Teor. Appl. 26: 3–28.

Gambino S, Barreca G, Gross F, Monaco C, Krastel S, Gutscher M.A. 2021. Deformation pattern of the northern sector of the Malta escarpment (Offshore SE Sicily, Italy): fault dimension, slip prediction, and seismotectonic implications. Front. Earth Sci. 8: 594176.

Gardiner W, Grasso M, Sedgeley D. 1995. Plio-Pleistocene fault movement as evidence for mega-block kinematics within the Hyblean—Malta Plateau, Central Mediterranean. J. Geodyn. 19(1): 35–51.

Gasparo Morticelli M, Valenti V, Catalano R, Sulli A, Agate M, Avellone G, Albanese C, Basilone L, Gugliotta C. 2015. Deep controls on foreland basin system evolution along the Sicilian fold and thrust belt. Bull. Soc. Géol. Fr. 186(4-5): 273–290.

Ghielmi M, Amore M.R., Bolla E.M., Carubelli P, Knezaurek G, Serraino C. 2012. The Pliocene to Pleistocene succession of the Hyblean foredeep (Sicily, Italy). In: AAPG Internat. Conf. Exhib. Milan, Italy, October (Vol. 23, p. 26).

Govers R, Wortel M.J.R. 2005. Lithosphere tearing at STEP faults: Response to edges of subduction zones. Earth Planet. Sci. Lett. 236(1-2): 505–523.

Grasso M, Reuther CD. 1988. The western margin of the Hyblean Plateau a neotectonic transform system on the SE Sicilian foreland. Ann. Tect. 2: 107–120.

Grasso M, Pedley MH, Reuther CD. 1985. The geology of the Pelagian Islands and their structural setting related to the Pantelleria rift (central Mediterranean Sea). CENTRO 1(2): 1-19.

Grasso M, Torelli L, Mazzoldi G. 1999. Cretaceous–Palaeogene sedimentation patterns and structural evolution of the Tunisian shelf, offshore the Pelagian islands (central Mediterranean). Tectonophysics 315(1-4): 235-250.

Guidoboni, E., Ferrari, G., Mariotti, D., Comastri, A., Tarabusi, G., Valensise, G. (2007). CFTI4Med, Catalogue of Strong Earthquakes in Italy (461 B.C.-1997) and Mediterranean Area (760 B.C.-1500). INGV-SGA, http://storing.ingv.it/cfti4med/.

Güneş P, Aksu AE, Hall J. 2018. Tectonic and sedimentary conditions necessary for the deposition of the Messinian evaporite successions in the eastern Mediterranean: A simple 2D model. Marine and Petroleum Geology 96: 51-70. https://doi.org/10.1016/j.marpetgeo.2018.05.022

Haq B, Gorini C, Baur J, Moneron J, Rubino JL. 2020. Deep Mediterranean's Messinian evaporite giant: How much salt? Global and Planetary Change 184: 103052.

Handy, M.R., Schmid, M.S., Bousquet, R., Kissling, E., Bernoulli, D., 2010. Reconciling plate-tectonic reconstructions of Alpine Tethys with the geological–geophysical record of spreading and subduction in the Alps. Earth Sci. Rev. 102, 121–158. https://doi.org/10.1016/j.earscirev.2010.06.002.

Holland CW, Etiope G, Milkov AV, Michelozzi E, Favali P. 2003. Mud volcanoes discovered offshore Sicily. Marine Geology 199(1-2): 1-6.

Imbò G. 1965. Catalogue of the active volcanoes of the world, Italy (Vol. 18). Rome: IAVCEI.

Innangi S, Tonielli R, Romagnoli C, Budillon F, Di Martino G, Innangi M, Laterza R, Le Bas T, Lo Iacono C. 2019. Seabed mapping in the Pelagie Islands marine protected area (Sicily Channel, southern Mediterranean) using remote sensing object based image analysis (RSOBIA). Marine Geophysical Research 40: 333-355.

ISIDe Working Group. 2007. Italian Seismological Instrumental and Parametric Database (ISIDe) (Version 1). National Institute of Geophysics and Volcanology (INGV). https://doi.org/10.13127/ISIDE

Jolivet L, Baudin T, Calassou S, Chevrot S, Ford M, Issautier B, Lasseur E, Masini E, Manatschal G, Mouthereau F, Thinon I. 2021. Geodynamic evolution of a wide plate boundary in the Western Mediterranean, near-field versus far-field interactions. BSGF-Earth Sciences Bulletin 192(1): 48.

Khomsi S, Jemia MGB, de Lamotte DF, Maherssi C, Echihi O, Mezni R. 2009. An overview of the Late Cretaceous–Eocene positive inversions and Oligo-Miocene subsidence events in the foreland of the Tunisian Atlas: Structural style and implications for the tectonic agenda of the Maghrebian Atlas system. Tectonophysics 475(1): 38-58.

Krijgsman W, Hilgen FJ, Raffi I, Sierro FJ, Wilson DS. 1999. Chronology, causes and progression of the Messinian salinity crisis. Nature 400(6745): 652-655.

Kuhlmann J, Asioli A, Trincardi F, Klügel A, Huhn K. 2017. Landslide frequency and failure mechanisms at NE Gela Basin (Strait of Sicily). Journal of Geophysical Research: Earth Surface 122(11): 2223-2243.

Lanzafame AC. 1994. SiII resonance multiplets in the Sun. Astronomy and Astrophysics 287: 972-981.

Le Breton E, Handy MR, Molli G, Ustaszewski K. 2017. Post-20 Ma motion of the Adriatic Plate: New constraints from surrounding orogens and implications for crust-mantle decoupling. Tectonics 36(12): 3135-3154. https://doi.org/10.1002/2016TC004443

Le Breton, E., Brune, S., Ustaszewski, K., Zahirovic, S., Seton, M., Müller, R.D., 2021. Kinematics and extent of the Piemont–Liguria Basin – implications for subduction processes in the Alps. Solid Earth 12, 885–913. https://doi.org/10.5194/se-12-885- 2021.

Lentini F, Carbone S, Catalano S, Monaco C. 1990. Tettonica a thrust neogenica nella Catena Appenninico-Maghrebide: esempi dalla Lucania e dalla Sicilia. Studi Geol. Camerti Vol. speciale: 19–26.

Lentini F, Carbone S, Catalano S. 1994. Main structural domains of the central Mediterranean region and their Neogene tectonic evolution. Boll. Geof. Teor. Appl. 36: 103–125.

Lentini F, Catalano S, Carbone S. 1996. The external thrust system in southern Italy; a target for petroleum exploration. Petroleum Geoscience 2(4): 333–342. doi:10.1144/petgeo.2.4.333

Lickorish WH, Grasso M, Butler RW, Argnani A, Maniscalco R. 1999. Structural styles and regional tectonic setting of the “Gela Nappe” and frontal part of the Maghrebian thrust belt in Sicily. Tectonics 18(4): 655-668.

Lodolo E, Civile D, Zanolla C, Geletti R. 2012. Magnetic signature of the Sicily Channel volcanism. Marine Geophysical Research 33: 33-44.

Lodolo E, Loreto MF, Melini D, Spada G, Civile D. 2022. Palaeo-shoreline configuration of the Adventure Plateau (Sicilian channel) at the last glacial maximum. Geosciences 12(3): 125.

Lodolo E, Civile D, Zecchin M, Zampa LS, Accaino F. 2019. A series of volcanic edifices discovered a few kilometers off the coast of SW Sicily. Marine Geology 416: 105999. https://doi.org/10.1016/j.margeo.2019.105999.

Lofi J, Sage F, Déverchère J, Loncke L, Maillard A, Gaullier V, Thinon I, Gillet H, Guennoc P, Gorini C. 2011. Refining our knowledge of the Messinian salinity crisis records in the offshore domain through multi-site seismic analysis. Bulletin de la Société géologique de France 182(2): 163-180.

Maesano, F.E., Tiberti, M.M., Basili, R., 2017. The Calabrian Arc: Three-dimensional modelling of the subduction interface. Sci. Rep. 7 (1), 1–15. https://doi.org/10.1038/s41598-017-09074-8.

Mahood G, Hildreth W. 1983. Large partition coefficients for trace elements in high-silica rhyolites. Geochimica et Cosmochimica Acta 47(1): 11-30. https://doi.org/10.1016/0016-7037(83)90087-X.

Maiorana M, Artoni A, Le Breton E, Sulli A, Chizzini N, Torelli L. 2023. Is the Sicily Channel a simple Rifting Zone? New evidence from seismic analysis with geodynamic implications. Tectonophysics 864: 230019.

Maiorana M, Spatola D, Todaro S, Caldareri F, Parente F, Severini A, Sulli A. 2024. Seismo-stratigraphic and morpho-bathymetric analysis revealing recent fluid-rising phenomena on the Adventure Plateau (northwestern Sicily Channel). Marine Geophysical Research 45(3): 15.

Manzi V, Argnani A, Corcagnani A, Lugli S, Roveri M. 2020. The Messinian salinity crisis in the Adriatic foredeep: evolution of the largest evaporitic marginal basin in the Mediterranean. Marine and Petroleum Geology 115: 104288.

Manzi V, Roveri M, Argnani A, Cowan D, Lugli S. 2021. Large-scale mass-transport deposits recording the collapse of an evaporitic platform during the Messinian salinity crisis (Caltanissetta basin, Sicily). Sedimentary Geology 424: 106003.

Minelli, L., Faccenna, C., 2010. Evolution of the Calabrian accretionary wedge (central Mediterranean). Tectonics 29. https://doi.org/10.1029/2009TC002562. TC 4004.

Chaumillon E, Mascle J. 1997. From foreland to forearc domains: new multichannel seismic reflection survey of the Mediterranean Ridge accretionary complex (Eastern Mediterranean). Marine Geology 138(3-4): 237-259.

Masrouhi A, Ghanmi M, Slama MMB, Youssef MB, Vila JM, Zargouni F. 2008. New tectono-sedimentary evidence constraining the timing of the positive tectonic inversion and the Eocene Atlasic phase in northern Tunisia: implication for the North African paleo-margin evolution. Reports. Geoscience 340(11): 771-778.

Meccariello M, Ferranti L, Barreca G, Palano M. 2017. New insights on the tectonics of the Lampedusa Plateau from the integration of offshore, onland and space geodetic data. Ital. J. Geosci. 136: 1–42. https://doi.org/10.3301/IJG.2017.02.

Micallef A, Camerlenghi A, Garcia-Castellanos D, Cunarro Otero D, Gutscher MA, Barreca G, Spatola D, Facchin L, Geletti R, Krastel S, Gross F. 2018. Evidence of the Zanclean megaflood in the eastern Mediterranean Basin. Scientific Reports 8(1): 1-8.

Micallef A, Geldmacher J, Watt SF, Ferrante GM, Ford J, Lodolo E, Civile D, Hodgetts AG, Felgendreher M, Licari JG, Hauff F. 2024. Submarine volcanism in the Sicilian Channel revisited. Marine Geology: 107342. https://doi.org/10.1016/j.margeo.2024.107342

Milia A, Iannace P, Torrente MM. 2021. The meeting place of backarc and foreland rifting: The example of the offshore western Sicily (Central Mediterranean). Global and Planetary Change 198: 103408.

Mueller C, Micallef A, Spatola D, Wang X. 2020. The tsunami inundation hazard of the Maltese Islands (central Mediterranean Sea): A submarine landslide and earthquake tsunami scenario study. Pure and Applied Geophysics 177: 1617-1638.

Nalpas T, Le Douaran S, Brun JP, Unternehr P, Richert JP. 1995. Inversion of the Broad Fourteens Basin (offshore Netherlands), a small-scale model investigation. Sedimentary Geology 95(3-4): 237-250.

Pace P, Scisciani V, Calamita F, Butler RW, Iacopini D, Esestime P, Hodgson N. 2015. Inversion structures in a foreland domain: seismic examples from the Italian Adriatic Sea. Interpretation. 3(4):SAA161-76.

Palano M, Ferranti L, Monaco C, Mattia M, Aloisi M, Bruno V, Cannavò F, Siligato G. 2012. GPS velocity and strain fields in Sicily and southern Calabria, Italy: Updated geodetic constraints on tectonic block interaction in the central Mediterranean. Journal of Geophysical Research: Solid Earth 117(B7). https://doi.org/10.1029/2012JB009254

Palano M, Ursino A, Spampinato S, Sparacino F, Polonia A, Gasperini L. 2020. Crustal deformation, active tectonics and seismic potential in the Sicily Channel (Central Mediterranean), along the Nubia–Eurasia plate boundary. Scientific Reports 10(1): 21238.

Panzera F, Lombardo G, Sicali S, D'Amico S. 2017. Surface geology and morphologic effects on seismic site response: The study case of Lampedusa, Italy. Physics and Chemistry of the Earth, Parts A/B/C 98: 62-72.

Peccerillo A. 2005. Plio-quaternary volcanism in Italy (Vol. 365). New York: Springer-Verlag Berlin Heidelberg.

Pellegrino AG, Maniscalco R, Speranza F, Hernandez-Moreno C, Sturiale G. 2016. Paleomagnetism of the Hyblean Plateau, Sicily: a review of the existing data set and new evidence for lack of block rotation from the Scicli-Ragusa Fault System. Italian Journal of Geosciences 135(2): 300-307.

Pellen R, Aslanian D, Rabineau M, Suc JP, Cavazza W, Popescu SM, Rubino JL. 2022. Structural and sedimentary origin of the Gargano-Pelagosa gateway and impact on sedimentary evolution during the Messinian Salinity Crisis. Earth-Science Reviews 232: 104114. https://doi.org/10.1016/j.earscirev.2022.104114

Pérez-Gussinyé M, Collier JS, Armitage JJ, Hopper JR, Sun Z, Ranero CR. 2023. Towards a process-based understanding of rifted continental margins. Nature Reviews Earth & Environment 4(3): 166-184.

Polonia A, Torelli L, Mussoni P, Gasperini L, Artoni A, Klaeschen D. 2011. The Calabrian Arc subduction complex in the Ionian Sea: Regional architecture, active deformation, and seismic hazard. Tectonics 30(5).

Polonia, A., Torelli, L., Gasperini, L., Mussoni, P., 2012. Active faults and historical earthquakes in the Messinian strait area (Ionian Sea). Nat. Hazards Earth Syst. Sci. 12, 2311–2328. https://doi.org/10.5194/nhess-12-2311-2012.

Ragg S, Grasso M, Müller B. 1999. Patterns of tectonic stress in Sicily from borehole breakout observations and finite element modeling. Tectonics 18(4): 669-685.

Richardson RM. 1992. Ridge forces, absolute plate motions, and the intraplate stress field. Journal of Geophysical Research: Solid Earth 97(B8): 11739-11748.

Rigane A, Gourmelen C. 2011. Inverted intracontinental basin and vertical tectonics: The Saharan Atlas in Tunisia. Journal of African Earth Sciences 61(2): 109-128.

Romagnoli C, Belvisi V, Innangi S, Di Martino G, Tonielli R. 2020. New insights on the evolution of the Linosa volcano (Sicily Channel) from the study of its submarine portions. Marine Geology 419: 106060.

Rooney TO. 2017. The Cenozoic magmatism of East-Africa: Part I—Flood basalts and pulsed magmatism. Lithos 286: 264-301.

Rosenbaum G, Weinberg RF, Regenauer-Lieb K. 2008. The geodynamics of lithospheric extension. Tectonophysics 458(1-4): 1-8.

Rotolo SG, Castorina F, Cellura D, Pompilio M. 2006. Petrology and geochemistry of submarine volcanism in the Sicily Channel Rift. The Journal of Geology 114(3): 355-365.

Roveri M, Flecker R, Krijgsman W, Lofi J, Lugli S, Manzi V, Sierro FJ, Bertini A, Camerlenghi A, De Lange G, Govers R. 2014. The Messinian Salinity Crisis: Past and future of a great challenge for marine sciences. Marine Geology 352: 25-58.

Royden L, Faccenna C. 2018. Subduction Orogeny and the Late Cenozoic Evolution of the Mediterranean Arcs. Annual Review of Earth and Planetary Sciences 46: 261–289. https://doi.org/10.1146/annurev-earth-060115-012419.

Scisciani V. 2009. Styles of positive inversion tectonics in the Central Apennines and in the Adriatic foreland: Implications for the evolution of the Apennine chain (Italy). Journal of Structural Geology 31(11): 1276-1294.

Shillington K. Charles Warren: Royal Engineer in the Age of Empire. 2021. eBook Partnership.

Sibson RH. 1995. Selective fault reactivation during basin inversion: potential for fluid redistribution through fault-valve action. Geological Society, London, Special Publications 88(1): 3-19.

Scognamiglio, L., Tinti, E., Quintiliani, M. (2006). Time Domain Moment Tensor (TDMT) [Data set]. Istituto Nazionale di Geofisica e Vulcanologia (INGV). https://doi.org/10.13127/TDMT

Spatola D, Micallef A, Sulli A, Basilone L, Ferreri R, Basilone G, Bonanno A, Pulizzi M, Mangano S. 2018. The Graham Bank (Sicily Channel, central Mediterranean Sea): seafloor signatures of volcanic and tectonic controls. Geomorphology 318: 375-389. https://doi.org/10.1016/j.geomorph.2018.07.006.

Spampinato, S., Ursino, A., Barbano, M.S. et al. A Reappraisal of Seismicity and Eruptions of Pantelleria Island and the Sicily Channel (Italy). Pure Appl. Geophys. 174, 2475–2493 (2017). https://doi.org/10.1007/s00024-017-1550-x

Spatola D, Sulli A, Casalbore D, Chiocci FL. 2021. First evidence of contourite drifts in the North-Western Sicilian active continental margin (Southern Tyrrhenian Sea). Journal of Marine Science and Engineering 9(10): 1043.

Speranza, F., Hernandez-Moreno, C., Avellone, G., Gasparo Morticelli, M., Agate, M., Sulli, A., Di Stefano, E., 2018. Understanding paleomagnetic rotations in Sicily: Thrust versus strike-slip tectonics. Tectonics 37 (4), 1138–1158.

Stampfli, G.M., Borel, G.D., Cavazza, W., Mosar, J., Ziegler, P.A., 2001. Palaeotectonic and palaeogeographic evolution of the western Tethys and PeriTethyan domain (IGCP Project 369). Episodes 2001 (24), 222–228. https://doi.org/10.18814/ epiiugs/2001/v24i4/001.

Stampfli GM, Borel GD. 2004. The TRANSMED transects in space and time: constraints on the paleotectonic evolution of the Mediterranean domain. In: The TRANSMED Atlas. The Mediterranean region from crust to mantle: Geological and geophysical framework of the Mediterranean and the surrounding areas. Berlin, Heidelberg: Springer Berlin Heidelberg, 53-80.

Sulli A. 2000. Structural framework and crustal characteristics of the Sardinia Channel Alpine transect in the central Mediterranean. Tectonophysics 324(4): 321–336.

Sulli A, Morticelli MG, Agate M, Zizzo E. 2021. Active north-vergent thrusting in the northern Sicily continental margin in the frame of the quaternary evolution of the Sicilian collisional system. Tectonophysics 802: 228717.

Tonielli R, Innangi S, Di Martino G, Romagnoli C. 2019. New bathymetry of the Linosa volcanic complex from multibeam systems (Sicily Channel, Mediterranean Sea). Journal of Maps 15(2): 611-618. https://doi.org/10.1080/17445647.2019.1642807.

Torelli L, Grasso M, Mazzoldi G, Peis D. 1998. Plio–Quaternary tectonic evolution and structure of the Catania foredeep, the northern Hyblean Plateau and the Ionian shelf (SE Sicily). Tectonophysics 298(1-3): 209-221. https://doi.org/10.1016/S0040-1951(98)00185-1.

Torelli L, Zitellini N, Argnani A, Brancolini G, De Cillia C, Peis D, Tricart P. 1993. Sezione geologica crostale dall'avampaese Pelagiano al bacino di retroarco Tirrenico (Mediterraneo Centrale). Mem Soc Geol It 47:385–399.

Torelli L, Grasso M, Mazzoldi G, Peis D, Gori D. 1995. Cretaceous to Neogene structural evolution of the Lampedusa shelf (Pelagian Sea, Central Mediterranean). Terra Nova 7(2):200-12.

Underhill JR, Paterson S. 1998. Genesis of tectonic inversion structures: seismic evidence for the development of key structures along the Purbeck–Isle of Wight Disturbance. Journal of the Geological Society 155(6): 975-992.

Van Dijk G, Maars J, Andreetto F, Hernández-Molina FJ, Rodríguez-Tovar FJ, Krijgsman W. 2023. A terminal Messinian flooding of the Mediterranean evidenced by contouritic deposits on Sicily. Sedimentology 70: 1195–1223. https://doi.org/10.1111/sed.13074.

van Dijk G, Maars J, Andreetto F, Hernández-Molina FJ, Rodríguez-Tovar FJ, Krijgsman W. A. 2023. Terminal Messinian flooding of the Mediterranean evidenced by contouritic deposits on Sicily. Sedimentology. 70(4):1195-223.

Van Hinsbergen, D.J.J., Torsvik, T.H., Schmid, S.M., Matenco, L.C., Maffione, M., Vissers, R.L.M., Gürer, D., Spakman, W., 2020. Orogenic architecture of the Mediterranean region and kinematic reconstruction of its tectonic evolution since the Triassic. Gondwana Res. 81, 79–229. https://doi.org/10.1016/j.gr.2019.07.009

Viger A, Dominguez S, Mazzotti S, Peyret M, Henriquet M, Barreca G, Monaco C, Damon A. 2024. Interseismic and long-term deformation of southeastern Sicily driven by the Ionian slab roll-back. EGUsphere 2024: 1-44.

Volpi V, Civile D, Lodolo E, Romeo R, Accettella D, Accaino F, Ferrante GM. 2022. Seabed and shallow morphological setting of the western Sicilian Channel. Bulletin of Geophysics and Oceanography 63(3): 357-376. https://hdl.handle.net/20.500.14083/14502.

Wang Z, Liu L, Fu Y, Zhao L, Lin J, Jin Z, Zheng B. 2023. Multistage plate subduction controls intraplate volcanism and cratonic lithospheric thinning in Northeast Asia. Earth-Science Reviews: 104590.

Washington HS. 1909. ART. VIII.--The Submarine Eruptions of 1831 and 1891 near Pantelleria. American Journal of Science (1880-1910) 27(158): 131.

Williams GD, Powell CM, Cooper MA. 1989. Geometry and kinematics of inversion tectonics. Geological Society, London, Special Publications 44(1): 3-15.

Ziegler PA, Dèzes P. 2006. Crustal evolution of western and central Europe. Geological Society, London, Memoirs 32(1): 43-56.

Ziegler PA, Cloetingh S. 1994. Dynamic Processes Governing Development of Rifted Basins. Paris: Technip. https://doi.org/10.1016/S0012-8252(03)00041-2.

Ziegler PA, Cloetingh S, van Wees JD. 1995. Dynamics of intra-plate compressional deformation: the Alpine foreland and other examples. Tectonophysics 252(1-4): 7-59.

Zitellini N, Ranero CR, Loreto MF, Ligi M, Pastore M, D'Oriano F, Sallares V, Grevemeyer I, Moeller S, Prada M. 2020. Recent inversion of the Tyrrhenian Basin. Geology 48(2): 123-127. https://doi.org/10.1130/G46774.1.

Zoback ML, Zoback M, Watts A, Schubert G. 2007. Lithosphere stress and deformation. Treatise on Geophysics: 253-273.

Illustration captions

Fig. 1. Bathymetric map showing the main structural elements of the Sicily Channel region - ATF: Adventure Thrust Front; CGSFZ: Capo-Granitola Sciacca Fault Zone; SRFS: Scicli-Ragusa Fault System; ETF: Egadi Thrust Front; GTF: Gela Thrust Front; GTS: Gela Thrust System; NB: Nameless Bank; GB: Graham Bank; MB: Madrepore Bank; SF: Sciacca Fault; CG: Capo Granitola Fault; MAG: Madrepore Graben; MG: Malta Graben; LG: Linosa Graben; PG: Pantelleria Graben (after Maiorana et al., 2024, in: Gasparo Morticelli et al., 2015; Civile et al., 2018; Sulli et al., 2021). The localization of the study area is marked by a yellow dotted box. Bathymetry data from EMODnet (https://emodnet.ec.europa.eu/en); Inset structural map from Le Breton et al. (2021).

Fig. 2. (a) Historical (blue squares) and instrumental seismicity (circles, colored as function of the hypocentral depth) over the study area. Historical seismicity has been collected from the SHARE European Earthquake Catalogue (https://www.emidius.eu/SHEEC/) and Spampinato et

al. (2017) and cover the 1000-1985 time interval. Instrumental seismicity is from ISIDE INGV database (https://terremoti.ingv.it/iside; ISIDe Working Group, 2007) and cover the Jan. 1985 - Aug. 2024 time interval. Focal mechanisms are from the GCMT (https://www.globalcmt.org; Ekström et al., 2012) and the TDMT (https://terremoti.ingv.it/en/tdmt; Scognamiglio et al., 2006) catalogs. (b) Geodetic velocity field (blue arrows) referred to a fixed African plate frame. Other symbols are: (1) volcanic fields (from the EMODnet database; https://emodnet.ec.europa.eu); (2) volcanic centers (Wurtz et al., 2015; Lodolo et al., 2019). Abbreviations are as following: HP, Hyblean Plateau; GB, Graham Bank; NB, Nameless Bank; Li, Linosa; La, Lampedusa. The dashed line represents the European/African boundary (see also Fig. 1). Bathymetry data from EMODnet.

Fig. 3. Lithostratigraphic correlation chart along section profile A-B, located on lower left corner map; we refer to the International Chronostratigraphic Chart issued by IUGS-International Union of Geological Sciences, 2022 (www.iugs.org) for the age constraint of the Plio-Quaternary; for details see section 3 in the manuscript (after Antonelli et al., 1988). TCS: Top of carbonate; TR: Top of Ragusa fm.; BTF: Base of Terravecchia; TMS: Top of Miocene; U1: Unconformity 1; U2: Unconformity 2; U3: Unconformity 3.

Fig. 4: Meso-Cenozoic paleogeographic evolution of the central and eastern sectors of the northern side of the Sicily Channel; a) top Pliensbachian (Lower Jurassic), b) top Early Cretaceous, c) top Eocene, d) top Oligocene, e) top Serravallian, f) top Messinian; refer to the text for details (after Antonelli et al., 1988).

Fig. 5. (a) Summary stratigraphic columns of published stratigraphic interpretations from various sectors of the Sicily Channel considered in this work (Adventure Plateau, Capo-Granitola Sciacca Fault Zone, Pantelelria Graben, Malta Graben, Linosa Graben, Gela Foredeep Basin), showing the differentiation between Pre-Plio-Quaternary and Plio-Quaternary sequences, as well as the main unconformities as originally defined and named by the respective authors; refer to Tab. 3 in Suppl. Mat. for description of the main horizons; (b) Synthetic stratigraphic framework constructed in this study by integrating the stratigraphic schemes presented in (a). This unified framework has been applied to the different study areas discussed in this work, in order to enable a consistent and comparable interpretation of the stratigraphic architecture across the Sicily Channel (TCS: Top of Carbonate succession; TR: Top of Ragusa Fm.; BTF: Top of Terravecchia fm.; TMS: Top of Miocene).

Fig. 6. Available seismic dataset and boreholes in the study area, derived from the literature and open access database (ViDEPI). Red lines correspond to the seismic reflection profiles reported in this work. Bathymetry data derived from EMODnet (https://emodnet.ec.europa.eu/en). Crm: Corvina Mare 1; Eg: Egeria 1; LG; Linosa Graben; MG: Malta Graben; Oe: Orione est-1; Or1: Orlando-1; Or2: Orlando-2; Pa: Palma-1; PG: Pantelleria Graben; Piera-01, Paola est-01; Re: Remo Nord-1; Ri: Riccio Sud-01; Samanta-1; Ve: Venere-1.

Fig. 7. (a) Uninterpreted and (b) interpreted Seismic Line 1 through the Adventure Plateau, modified after Civile et al. (2014); see Fig. 6 for location, Fig. 5b and Tab. 3 in Suppl. Mat. for description of the main horizons (TCS: Top of Carbonate succession; BTF: Base of Terravechia fm.; TMS: Top of Miocene). Recent reactivation of the SE-verging Egadi Thrust Front (ETF) is

visible, as it affects the seafloor. Note that the uninterpreted line in (a), publicity available at www.videpi.com, was provided as already interpreted by AGIP-ENI S.p.A.

Fig. 8. (a) Uninterpreted and (a’) interpreted Seismic Line 2 and (b) uninterpreted and (b’) interpreted Seismic Line 3 through Sciacca Fault zone, modified after Fedorick et al. (2018), and publicity available at www.videpi.com; see Fig. 6 for location, Fig. 5b and Tab. 3 in Suppl. Mat. for description of the main horizons (TCS: Top of Carbonate succession; TMS: Top of Miocene). The profiles show a positive flower structure associated with the Sciacca Fault, deforming the Plio-Quaternary and Pre Plio-Quaternary strata. Dashed lines represent unconformities tentatively interpreted in this work, in accordance with the synthetic stratigraphic framework of the Sicily Channel shown in Fig. 5b.

Fig. 9. (a) Uninterpreted and (b) interpreted Seismic Line 4 through the Pantelleria Graben, modified after Civile et al. (2021); see Fig. 6 for location, Fig. 5b and Tab. 3 in Suppl. Mat. for description of the main horizons (TCS: Top of Carbonate succession; TMS: Top of Miocene). The southern termination of the Pantelleria Graben is shown with highlighted a possible positive tectonic inversion; the folding in the sedimentary Plio-Quaternary infill of the graben is linked to the existence of a supposed buried magmatic intrusion by Civile et al. (2021). Dashed lines represent unconformities tentatively interpreted in this work, in accordance with the synthetic stratigraphic framework of the Sicily Channel shown in Fig. 5b.

Fig. 10. (a) Uninterpreted and (a') interpreted Seismic Line 5 through Malta Graben and (b) uninterpreted and (b') interpreted Seismic Line 6 through Linosa Graben, modified after Maiorana et al. (2023); see Fig. 6 for location, Fig. 5b and Tab. 3 in Suppl. Mat. for the description of the main horizons (TCS: Top of Carbonate succession; TMS: Top of Miocene). Dashed lines represent unconformities tentatively interpreted in this work, in accordance with the synthetic stratigraphic framework of the Sicily Channel shown in Fig. 5b.

Fig. 11. (a) Uninterpreted and (b) interpreted Seismic Line 10 through the Gela Foredeep Basin, modified after Catalano et al. (1996) and publicity available at www.videpi.com; see Fig. 6 for location, Fig. 5b and Tab. 3 in Suppl. Mat. for description of the main horizons (TMS: Top of Miocene). The Gela Foredeep Basin extends south of the Gela Thrust System (GTS) as a weakly deformed depocenter, characterized by onlap termination against the GTS. The latter, marked by several SW-verging thrusts, clearly deforms the TMS and U3 horizons. Dashed lines represent unconformities tentatively interpreted in this work, by the synthetic stratigraphic framework of the Sicily Channel shown in Fig. 5b.

Fig. 12. (a) Uninterpreted and (a') interpreted Seismic Line 8 and (b) uninterpreted and (b') interpreted Seismic Line (b) through the Gela Foredeep Basin, modified after Cavallaro et al. (2017); see Fig. 6 for location, Fig. 5b and Tab. 3 in Suppl. Mat. for description of the main horizons (TCS: Top of Carbonate succession; TR: Top of Ragusa; TMS: Top of Miocene). In (a') the Gela Foredeep Basin, marked by onlap termination against the Gela Thrust System (GTS) and the Madrepore Bank; the latter is characterized by the absence of Plio-Quaternary sediments on its top and displays active extensional faults as they reach the seafloor; in (b')

the Gela Foredeep Basin and the Malta High, which is covered by a thin layer of Plio-Quaternary deposits and marked by a widespread extensional tectonics.

Fig. 13. Map compilation of all tectonic structures of Sicily Channel that have been active since Late Miocene time (for Late Miocene-Early Pliocene, see Fig. 13; for Pleistocene see Fig. 14; for Active see Fig. 15). CGSFZ: Capo-Granitola Sciacca Fault Zone; ETF: Egadi Thrust Front; GTF: Gela Thrust Front; IF; Inverted Fault; ATF: Adventure Thrust Front: SRFS: Scicly Ragusa Fault System; NF: Normal fault; TF: Thrust fault; SSF: Strike-Slip Fault. The shape files of all tectonic structures are provided in the supplementary materials.

Fig. 14. Map of the active Late Miocene-Early Pliocene structural features in the Sicily Channel derived from Fig. 12 (see section 6.1 for detail). CGSFZ: Capo-Granitola Sciacca Fault Zone; SRFS: Scicli-Ragusa Fault System; SMTF: Sicily-Maghrebian Thrust Front; ETF: Egadi Thrust Front; GTS: Gela Thrust Front; ATF: Adventure Thrust Front.

Fig. 15. Map of the active Early Pleistocene structural features in the Sicily Channel extracted from Fig 12 (detail in section 6.1). CGSFZ: Capo-Granitola Sciacca Fault Zone; SRFS: Scicli-Ragusa Fault System; ETF: Egadi Thrust Front; GTS: Gela Thrust Front.

Fig. 16. Map of the present day active structural features in the Sicily Channel, derived from Fig. 12 (refer to section 6.1 for detail). CGSFZ: Capo-Granitola Sciacca Fault Zone; SRFS: Scicli-Ragusa Fault System; ETF: Egadi Thrust Front.

Fig. 17. Schematic representation showing the tectonic events occurred in the Sicily Channel illustrating the competition between slab roll-back of the African plate and Africa-European plate convergence (after Argnani, 1990 and Maiorana et al., 2023); a) Late Miocene; b) Pliocene; c) Late Pleistocene; d) Present day; see the text for the explanations (modified after Argnani, 1990).

Figure 1

Figure 2

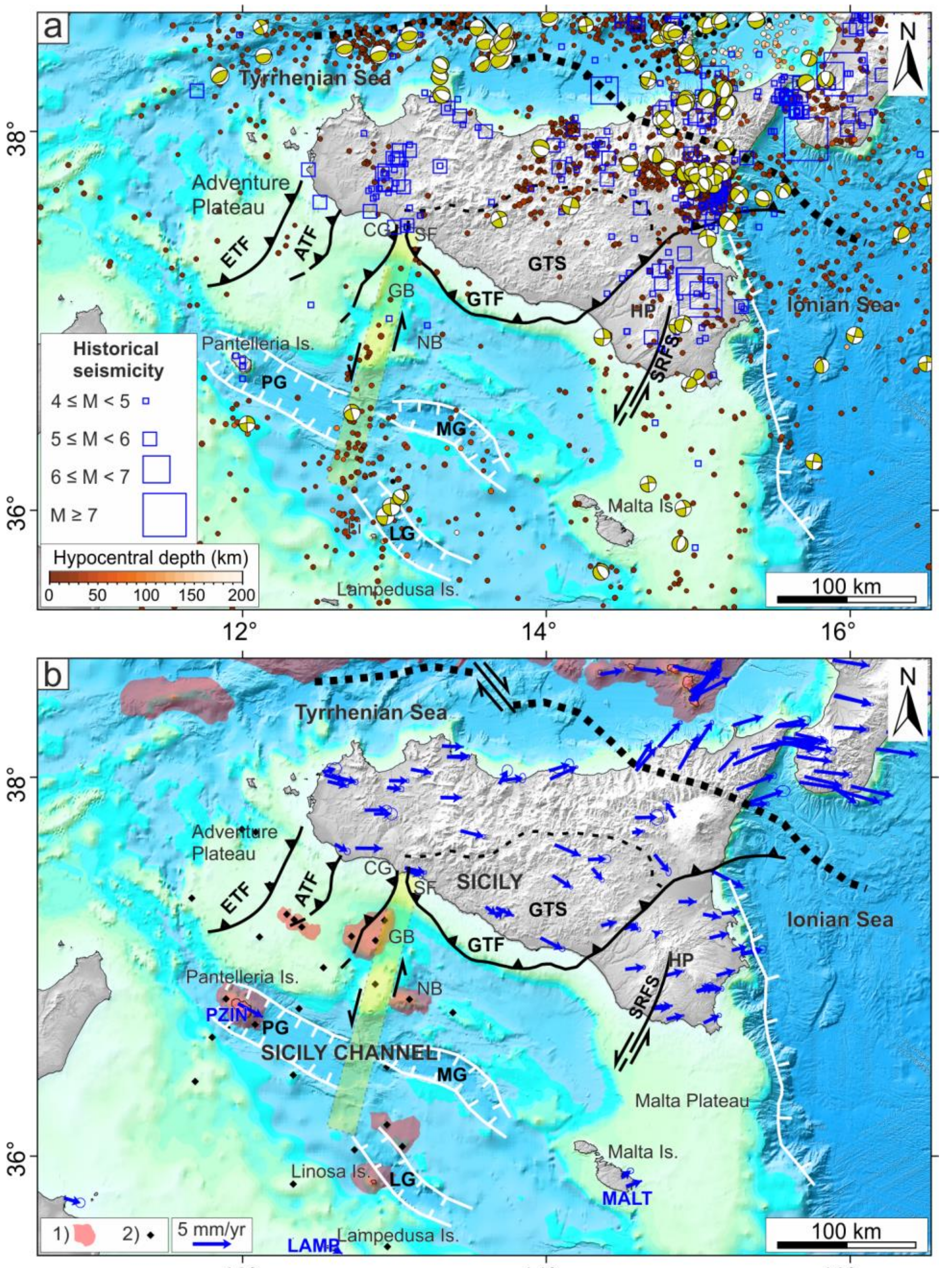
a
Tyrrhenian Sea
Adventure Plateau
ETF
ATF
CG
SF
GB
NB
GTS
GTF
HP
SRFS
Ionian Sea
Pantelleria Is.
PG
MG
LG
Malta Is.
Lampedusa Is.
Historical seismicity
4 ≤ M < 5
5 ≤ M < 6
6 ≤ M < 7
M ≥ 7
Hypocentral depth (km)
0 50 100 150 200
100 km
N
38°
36°
12°
14°
16°
b
Tyrrhenian Sea
Adventure Plateau
ETF
ATF
CG
SF
SICILY
GTS
GB
GTF
HP
SRFS
Ionian Sea
Pantelleria Is.
PZIN
PG
NB
SICILY CHANNEL
MG
Malta Plateau
Malta Is.
MALT
Linosa Is.
LG
Lampedusa Is.
LAMP
1)
2)
5 mm/yr
100 km
N
38°
36°
12°
14°
16°

Figure 3

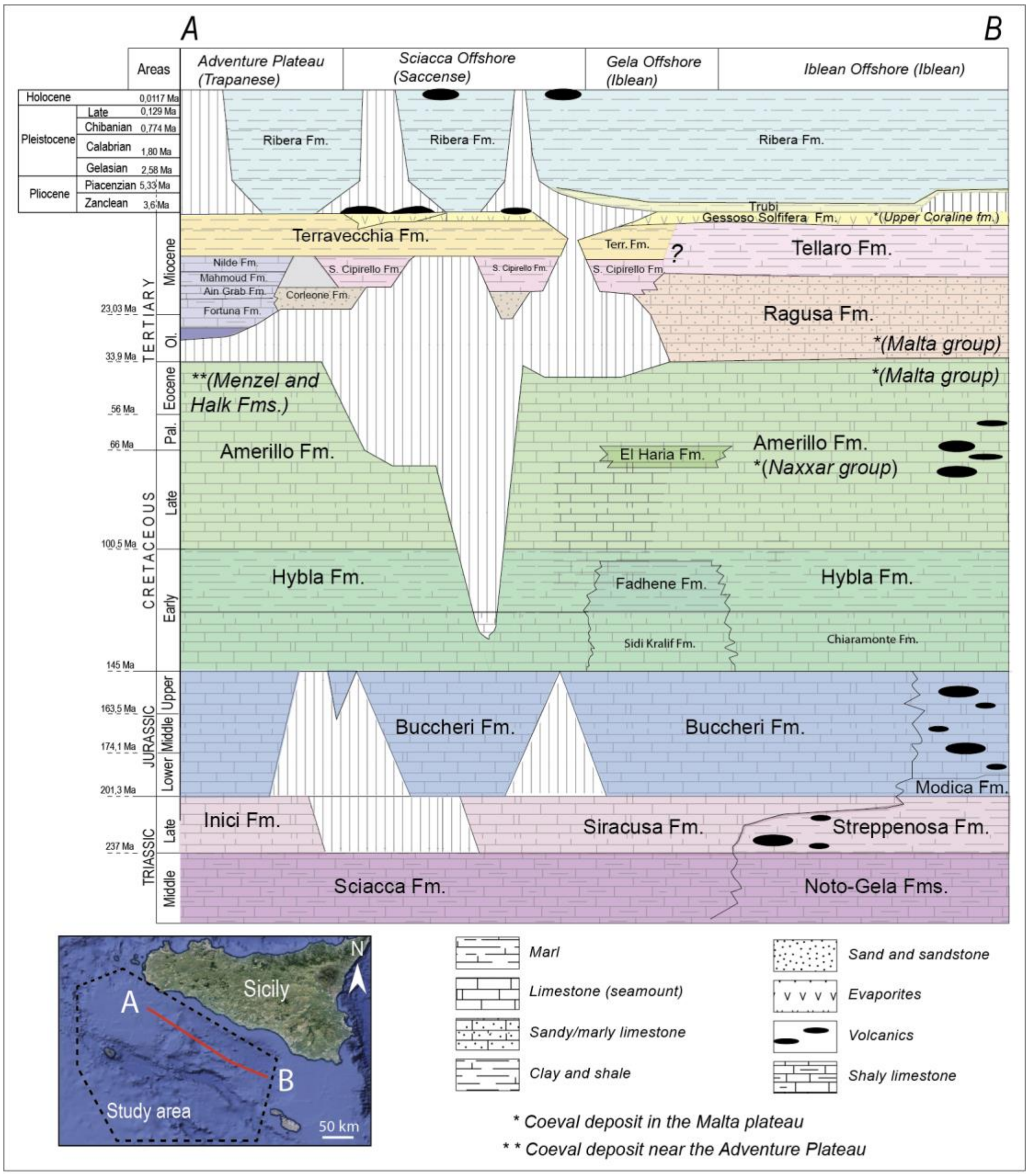

A
B
Areas
Adventure Plateau (Trapanese)
Sciacca Offshore (Saccense)
Gela Offshore (Iblean)
Iblean Offshore (Iblean)
Holocene
Late
Chibanian
Calabrian
Gelasian
Pleistocene
Pliocene
Piacenzian
Zanclean
TERTIARY
Miocene
Ol.
Eocene
Pal.
CRETACEOUS
Late
Early
JURASSIC
Upper
Middle
Lower
TRIASSIC
Late
Middle
23,03 Ma
33,9 Ma
56 Ma
66 Ma
100,5 Ma
145 Ma
163,5 Ma
174,1 Ma
201,3 Ma
237 Ma
Ribera Fm.
Ribera Fm.
Ribera Fm.
Trubi
Gessoso Solfifera Fm.
*(Upper Coraline fm.)
Terravecchia Fm.
Terr. Fm.
?
Tellaro Fm.
Nilde Fm.
Mahmoud Fm.
Ain Grab Fm.
Fortuna Fm.
Corleone Fm.
S. Cipirello Fm.
S. Cipirello Fm.
S. Cipirello Fm.
Ragusa Fm.
*(Malta group)
*(Malta group)
**(Menzel and Halk Fms.)
Amerillo Fm.
El Haria Fm.
Amerillo Fm.
*(Naxxar group)
Hybla Fm.
Fadhene Fm.
Hybla Fm.
Sidi Kralif Fm.
Chiaramonte Fm.
Buccheri Fm.
Buccheri Fm.
Modica Fm.
Inici Fm.
Siracusa Fm.
Streppenosa Fm.
Sciacca Fm.
Noto-Gela Fms.
N
Sicily
A
B
Study area
50 km
Marl
Limestone (seamount)
Sandy/marly limestone
Clay and shale
Sand and sandstone
Evaporites
Volcanics
Shaly limestone
* Coeval deposit in the Malta plateau
* * Coeval deposit near the Adventure Plateau

Figure 4

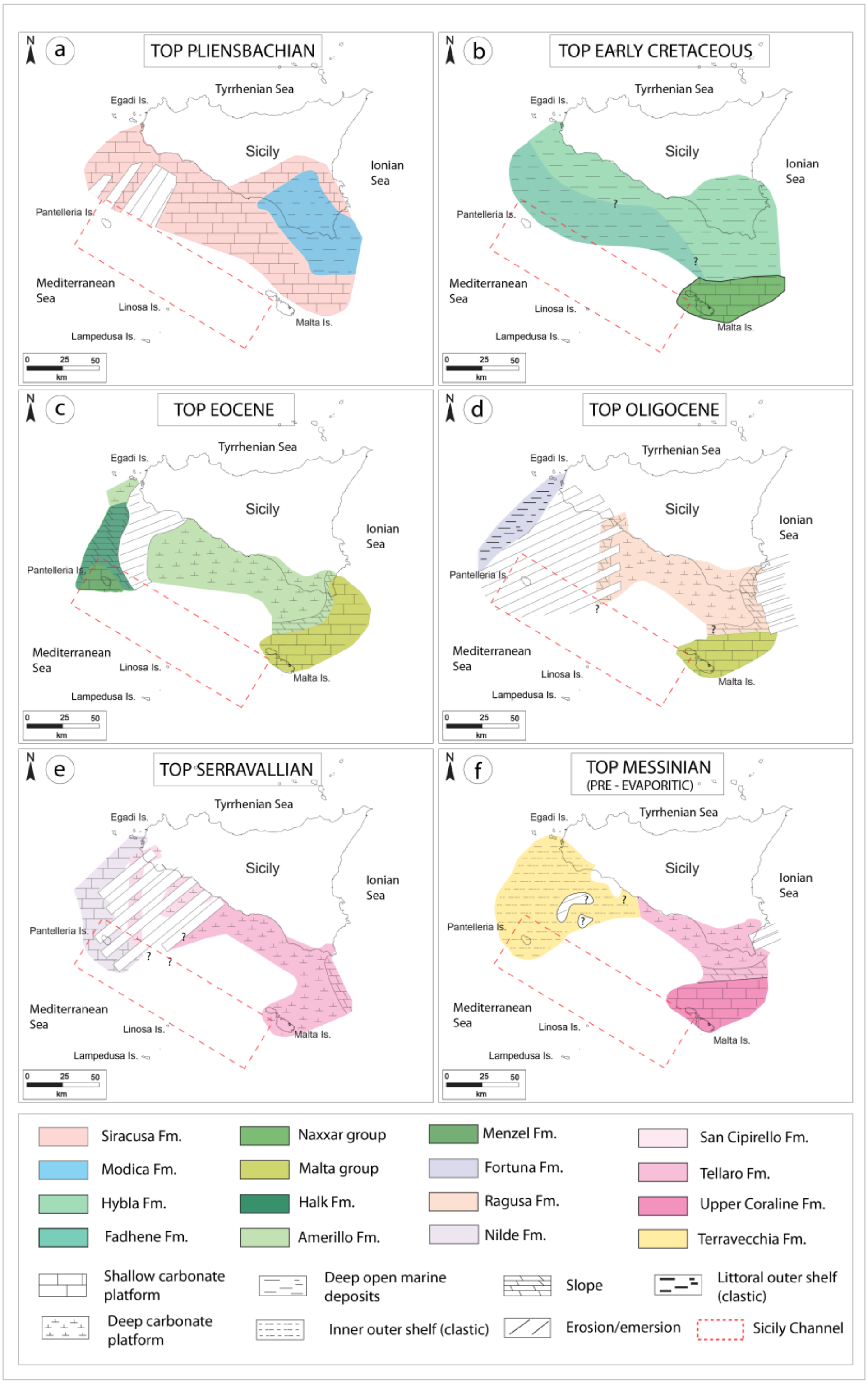
a
TOP PLIENSBACHIAN
b
TOP EARLY CRETACEOUS
c
TOP EOCENE
d
TOP OLIGOCENE
e
TOP SERRAVALLIAN
f
TOP MESSINIAN
(PRE - EVAPORITIC)
N
Tyrrhenian Sea
Egadi Is.
Sicily
Ionian Sea
Pantelleria Is.
Mediterranean Sea
Linosa Is.
Lampedusa Is.
Malta Is.
0 25 50 km
Siracusa Fm.
Modica Fm.
Hybla Fm.
Fadhene Fm.
Naxxar group
Malta group
Halk Fm.
Amerillo Fm.
Menzel Fm.
Fortuna Fm.
Ragusa Fm.
Nilde Fm.
San Cipirello Fm.
Tellaro Fm.
Upper Coraline Fm.
Terravecchia Fm.
Shallow carbonate platform
Deep carbonate platform
Deep open marine deposits
Inner outer shelf (clastic)
Slope
Erosion/emersion
Littoral outer shelf (clastic)
Sicily Channel

Figure 5

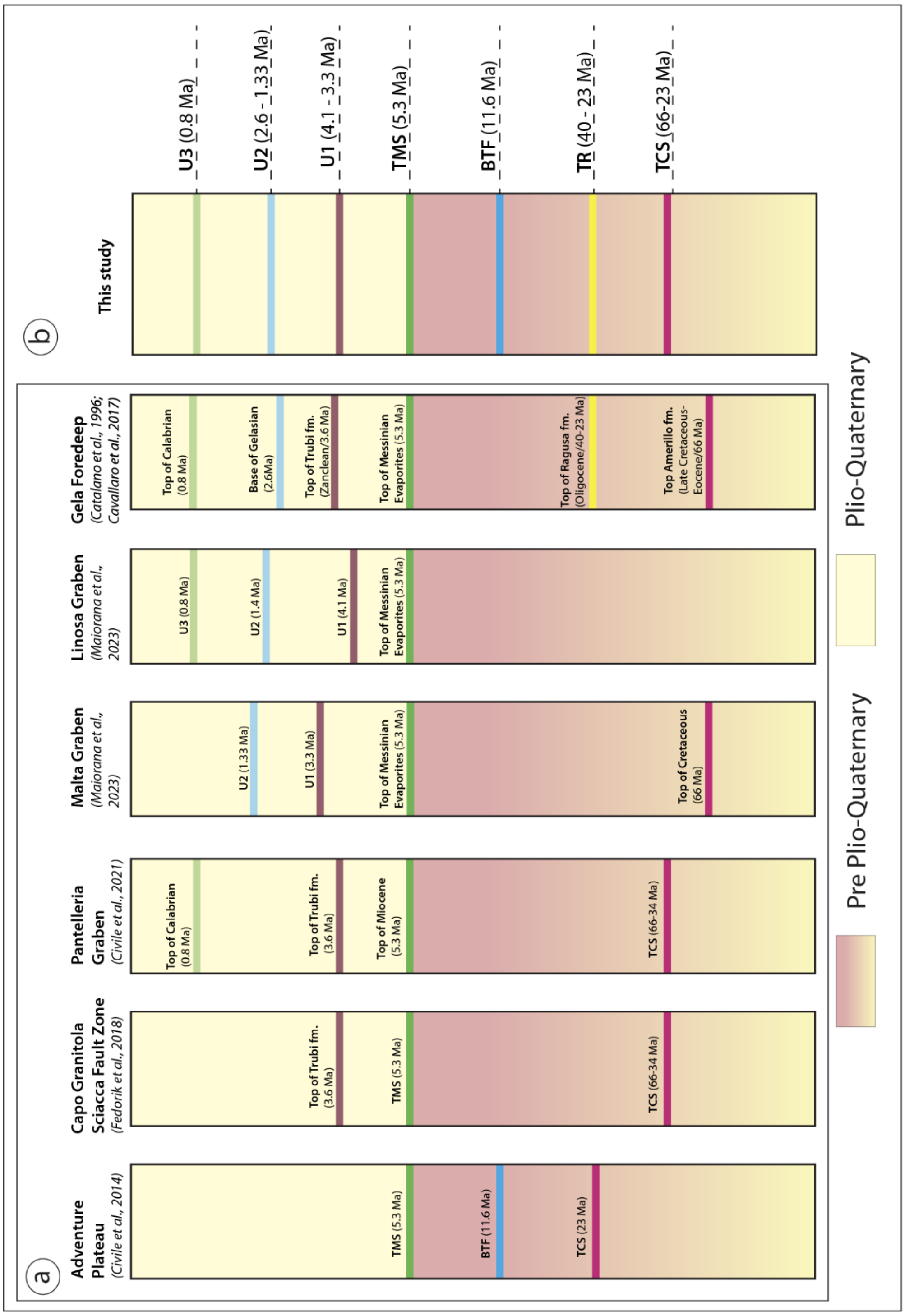
a
Adventure Plateau (Civile et al., 2014)
TMS (5.3 Ma)
BTF (11.6 Ma)
TCS (23 Ma)
Capo Granitola Sciacca Fault Zone (Fedorik et al., 2018)
Top of Trubi fm. (3.6 Ma)
TMS (5.3 Ma)
TCS (66-34 Ma)
Pantelleria Graben (Civile et al., 2021)
Top of Calabrian (0.8 Ma)
Top of Trubi fm. (3.6 Ma)
Top of Miocene (5.3 Ma)
TCS (66-34 Ma)
Malta Graben (Maiorana et al., 2023)
U2 (1.33 Ma)
U1 (3.3 Ma)
Top of Messinian Evaporites (5.3 Ma)
Top of Cretaceous (66 Ma)
Linosa Graben (Maiorana et al., 2023)
U3 (0.8 Ma)
U2 (1.4 Ma)
U1 (4.1 Ma)
Top of Messinian Evaporites (5.3 Ma)
Gela Foredeep (Catalano et al., 1996; Cavallaro et al., 2017)
Top of Calabrian (0.8 Ma)
Base of Gelasian (2.6Ma)
Top of Trubi fm. (Zanclean/3.6 Ma)
Top of Messinian Evaporites (5.3 Ma)
Top of Ragusa fm. (Oligocene/40-23 Ma)
Top Amerillo fm. (Late Cretaceous-Eocene/66 Ma)
b
This study
U3 (0.8 Ma)
U2 (2.6 - 1.33 Ma)
U1 (4.1 - 3.3 Ma)
TMS (5.3 Ma)
BTF (11.6 Ma)
TR (40 - 23 Ma)
TCS (66-23 Ma)
Pre Plio-Quaternary
Plio-Quaternary

Figure 6

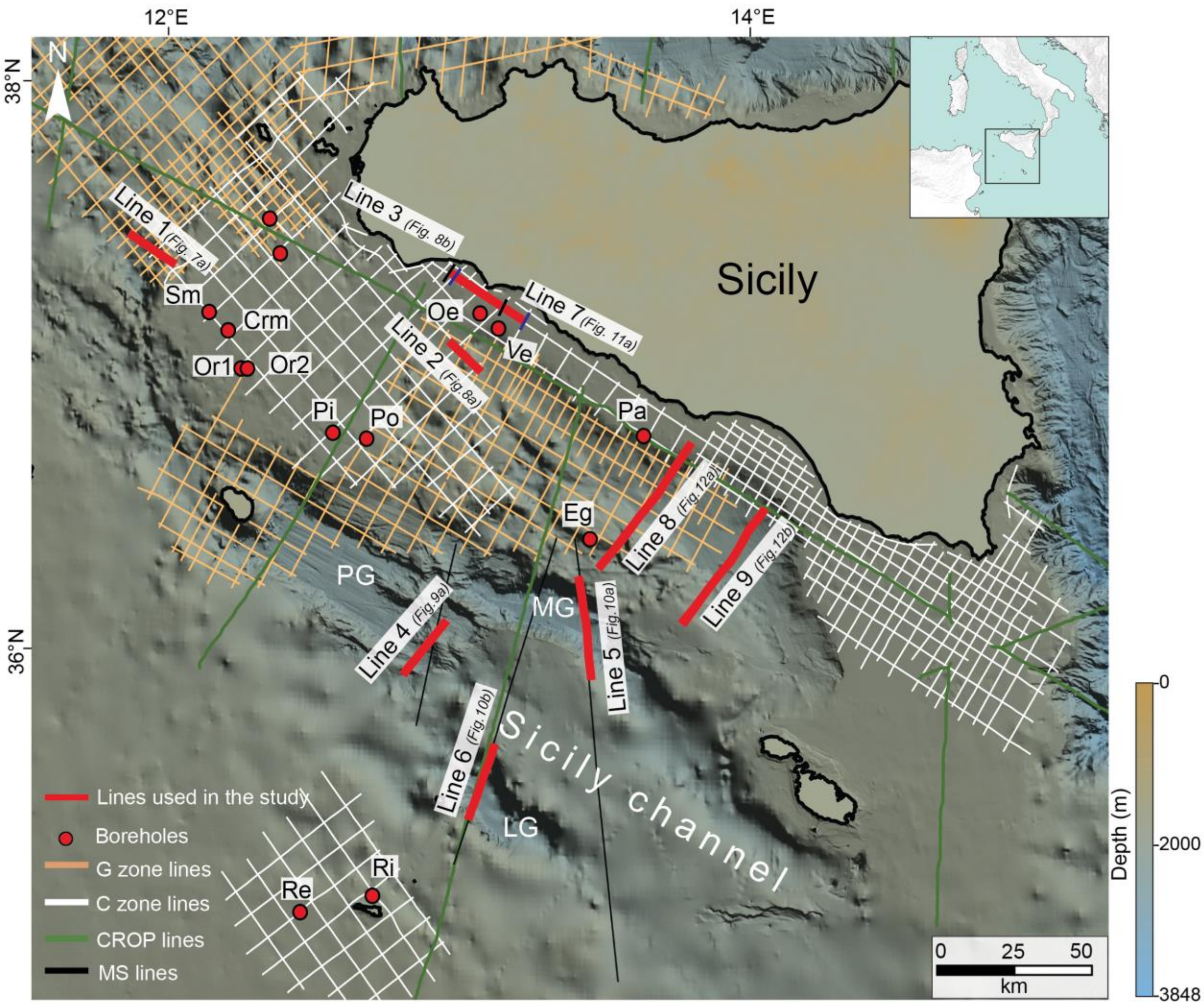
12°E
14°E
38°N
36°N
N
Sicily
Line 1 (Fig. 7a)
Line 2 (Fig. 8a)
Line 3 (Fig. 8b)
Line 4 (Fig. 9a)
Line 5 (Fig. 10a)
Line 6 (Fig. 10b)
Line 7 (Fig. 11a)
Line 8 (Fig. 12a)
Line 9 (Fig. 12b)
Sm
Crm
Or1
Or2
Oe
Ve
Pi
Po
Pa
Eg
Re
Ri
PG
MG
LG
Sicily channel
Lines used in the study
Boreholes
G zone lines
C zone lines
CROP lines
MS lines
0 25 50
km
Depth (m)
0
-2000
-3848

1404

Figure 7

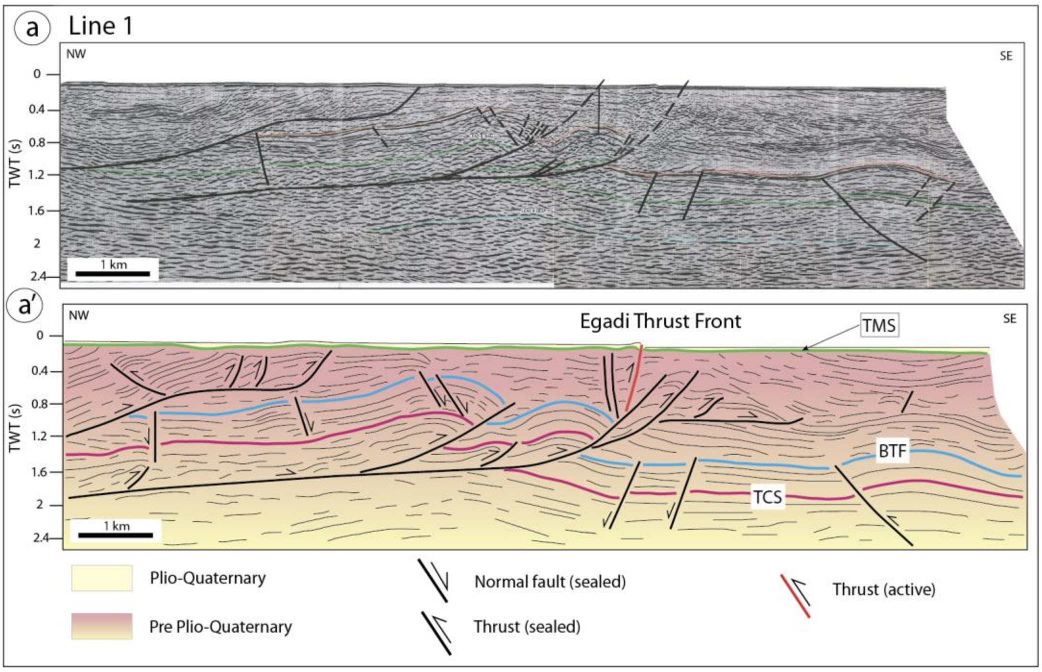

1405

1406

Figure 8

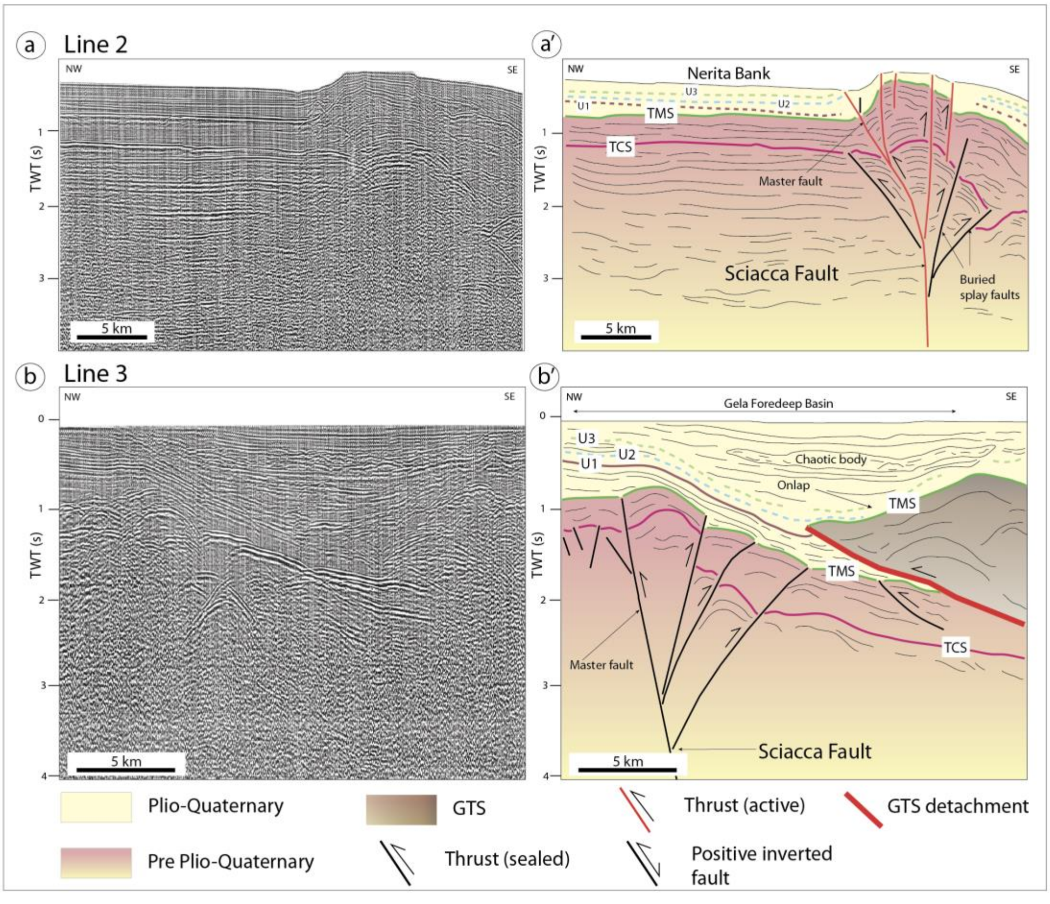

1407

Figure 9

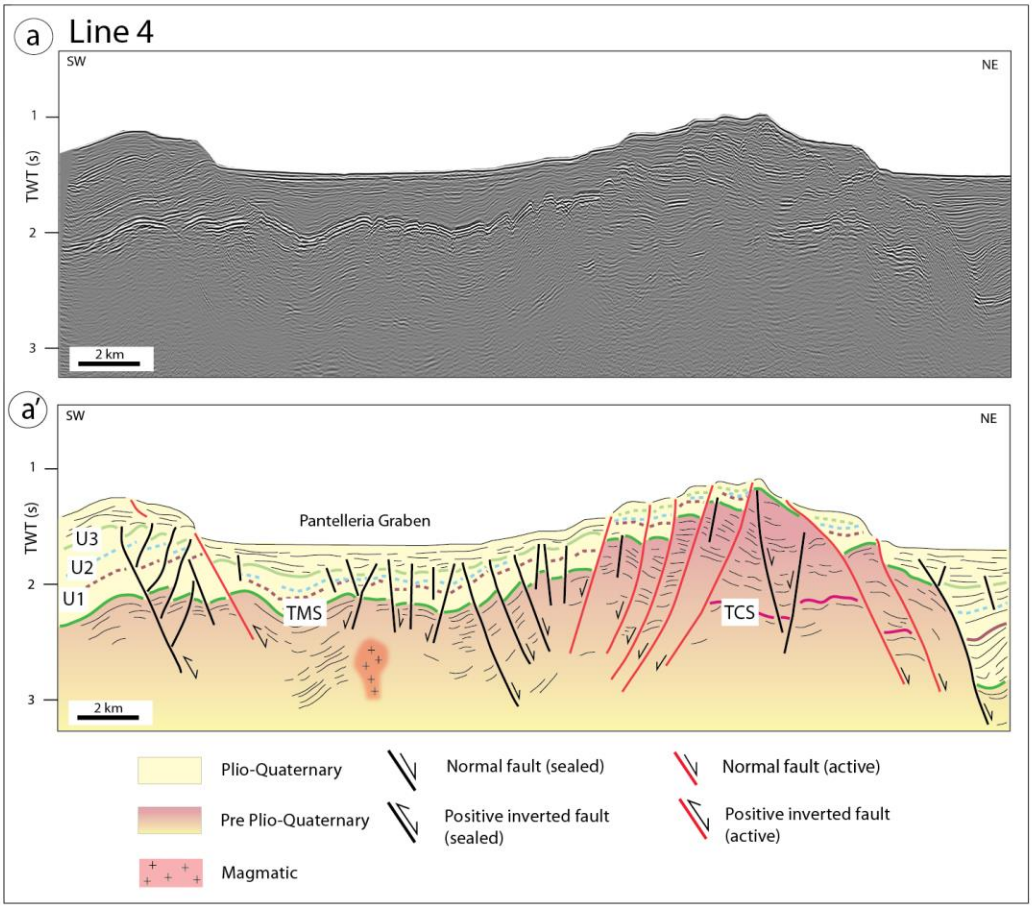

a
Line 4
SW
NE
TWT (s)
1
2
3
2 km
a'
SW
NE
TWT (s)
1
2
3
Pantelleria Graben
U3
U2
U1
TMS
TCS
2 km
Plio-Quaternary
Pre Plio-Quaternary
Magmatic
Normal fault (sealed)
Positive inverted fault (sealed)
Normal fault (active)
Positive inverted fault (active)

Figure 10

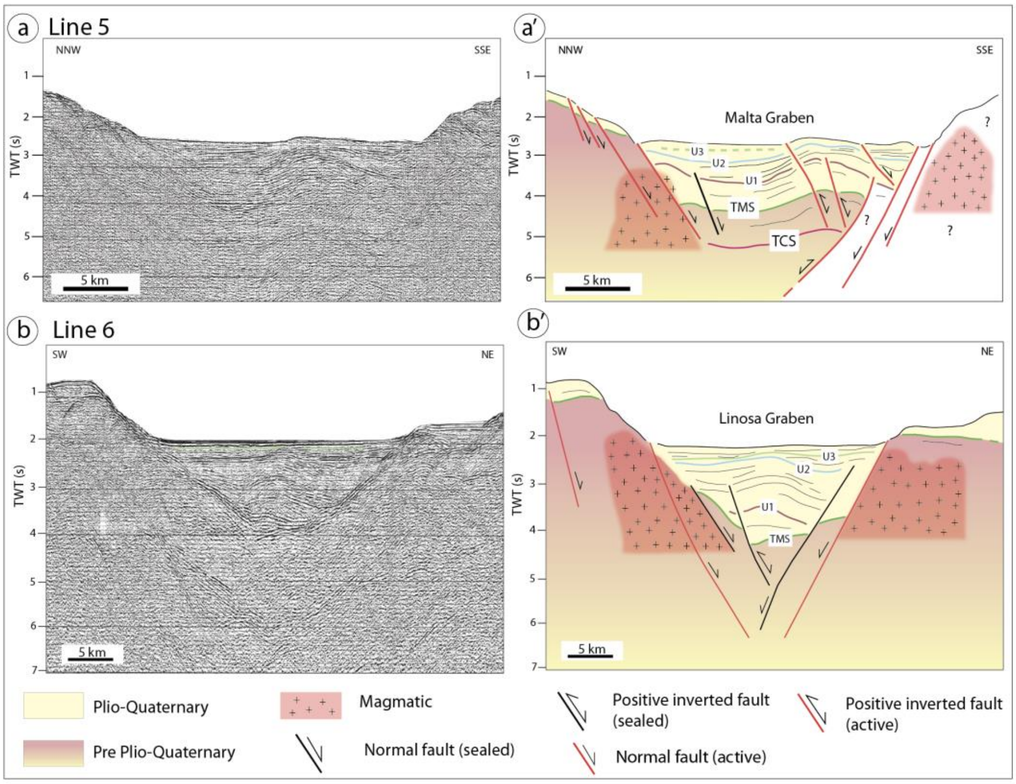

a Line 5
NNW
SSE
TWT (s)
5 km
a′
Malta Graben
U3
U2
U1
TMS
TCS
b Line 6
SW
NE
b′
Linosa Graben
Plio-Quaternary
Pre Plio-Quaternary
Magmatic
Normal fault (sealed)
Positive inverted fault (sealed)
Normal fault (active)
Positive inverted fault (active)

Figure 11

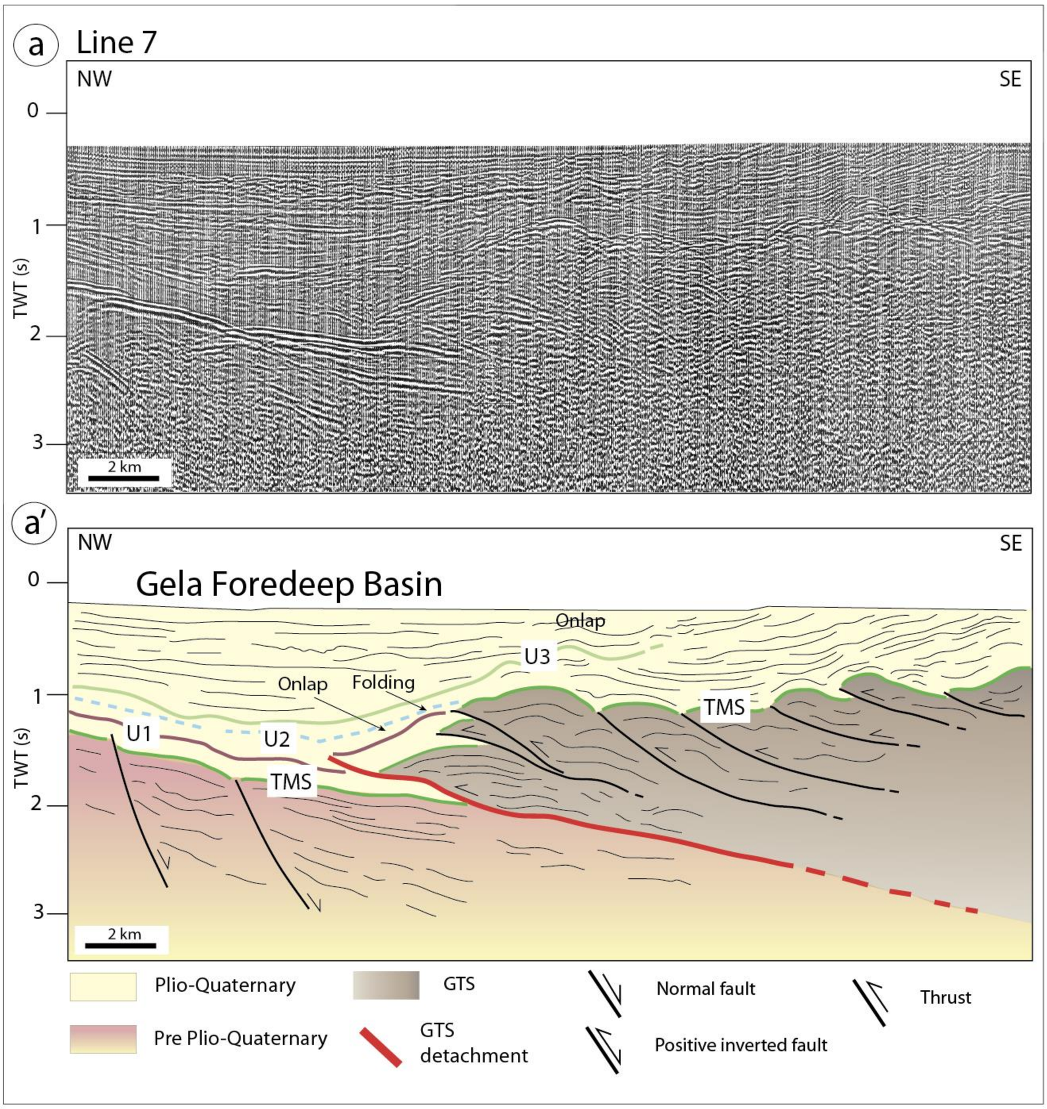

a
Line 7
NW
SE
0
1
2
3
TWT (s)
2 km
a′
NW
SE
Gela Foredeep Basin
Onlap
U3
Onlap
Folding
U1
U2
TMS
TMS
0
1
2
3
TWT (s)
2 km
Plio-Quaternary
GTS
Normal fault
Thrust
Pre Plio-Quaternary
GTS detachment
Positive inverted fault

Figure 12

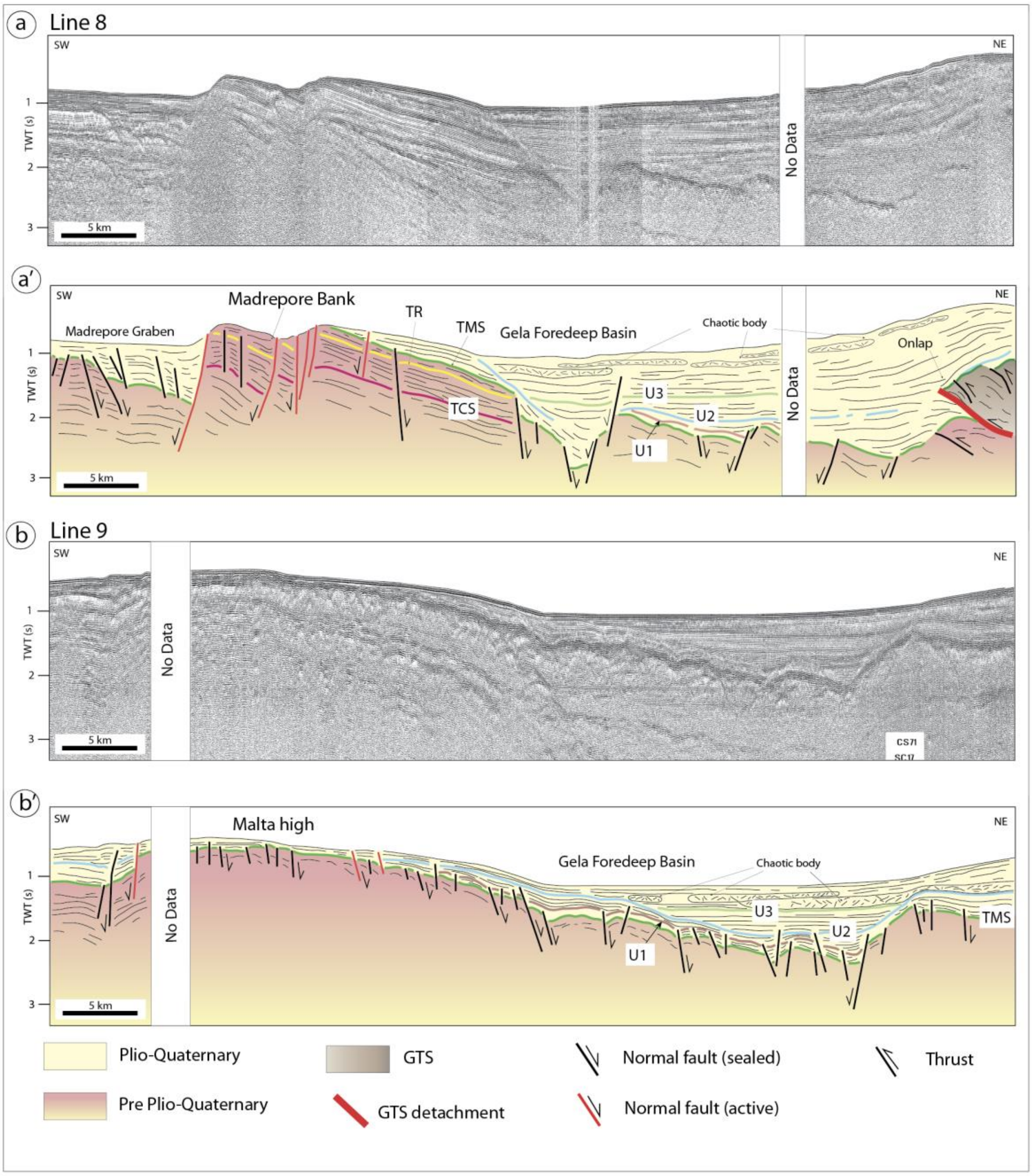
a
Line 8
SW
NE
TWT (s)
1
2
3
5 km
No Data
a′
Madrepore Bank
Madrepore Graben
TR
TMS
Gela Foredeep Basin
Chaotic body
Onlap
TCS
U3
U2
U1
b
Line 9
CS71
SC17
b′
Malta high
TMS
Plio-Quaternary
Pre Plio-Quaternary
GTS
GTS detachment
Normal fault (sealed)
Normal fault (active)
Thrust

Figure 13

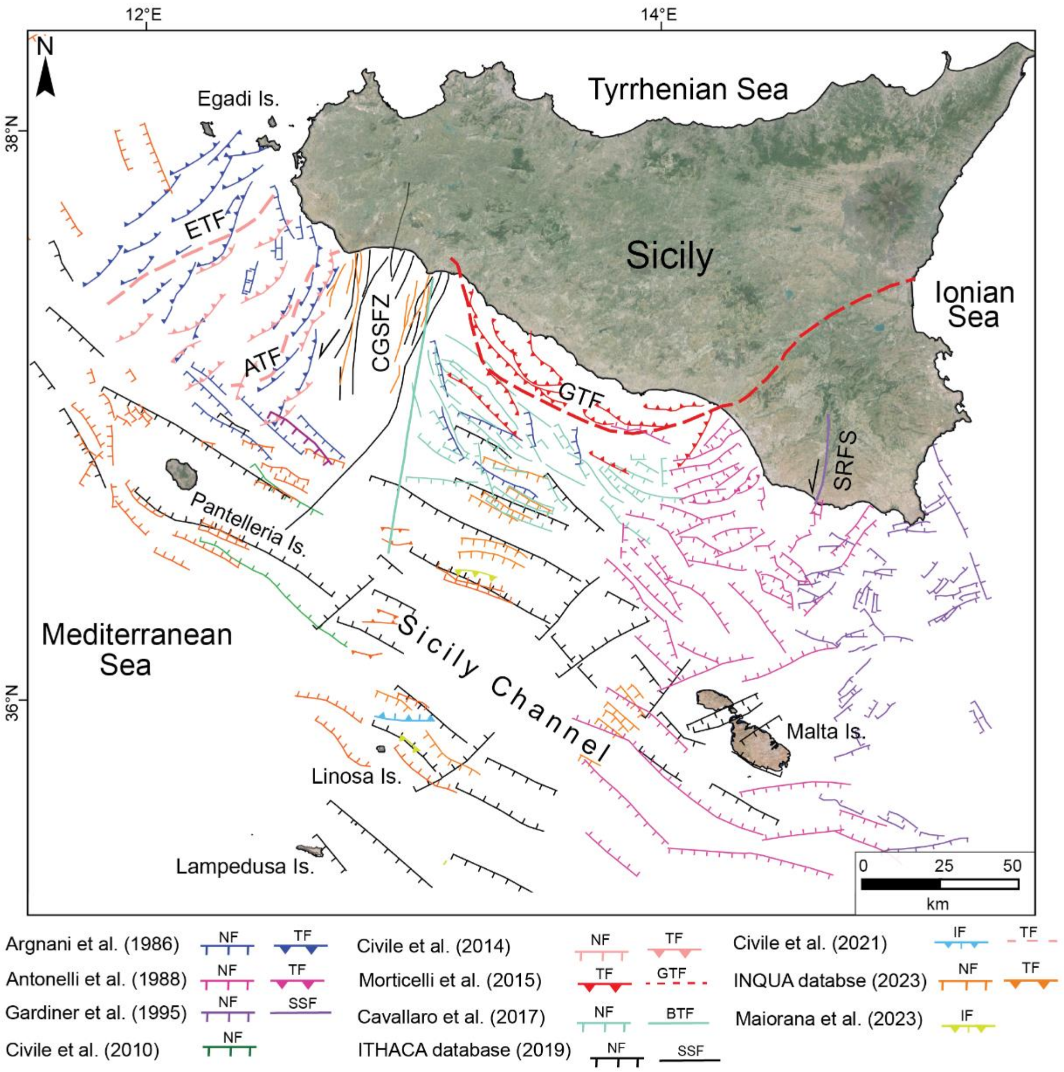

12°E
14°E
38°N
36°N
N
Egadi Is.
Tyrrhenian Sea
Sicily
Ionian Sea
ETF
ATF
CGSFZ
GTF
SRFS
Pantelleria Is.
Mediterranean Sea
Sicily Channel
Malta Is.
Linosa Is.
Lampedusa Is.
0 25 50
km
Argnani et al. (1986) NF TF
Antonelli et al. (1988) NF TF
Gardiner et al. (1995) NF SSF
Civile et al. (2010) NF
Civile et al. (2014) NF TF
Morticelli et al. (2015) TF GTF
Cavallaro et al. (2017) NF BTF
ITHACA database (2019) NF SSF
Civile et al. (2021) IF TF
INQUA databse (2023) NF TF
Maiorana et al. (2023) IF

Figure 14

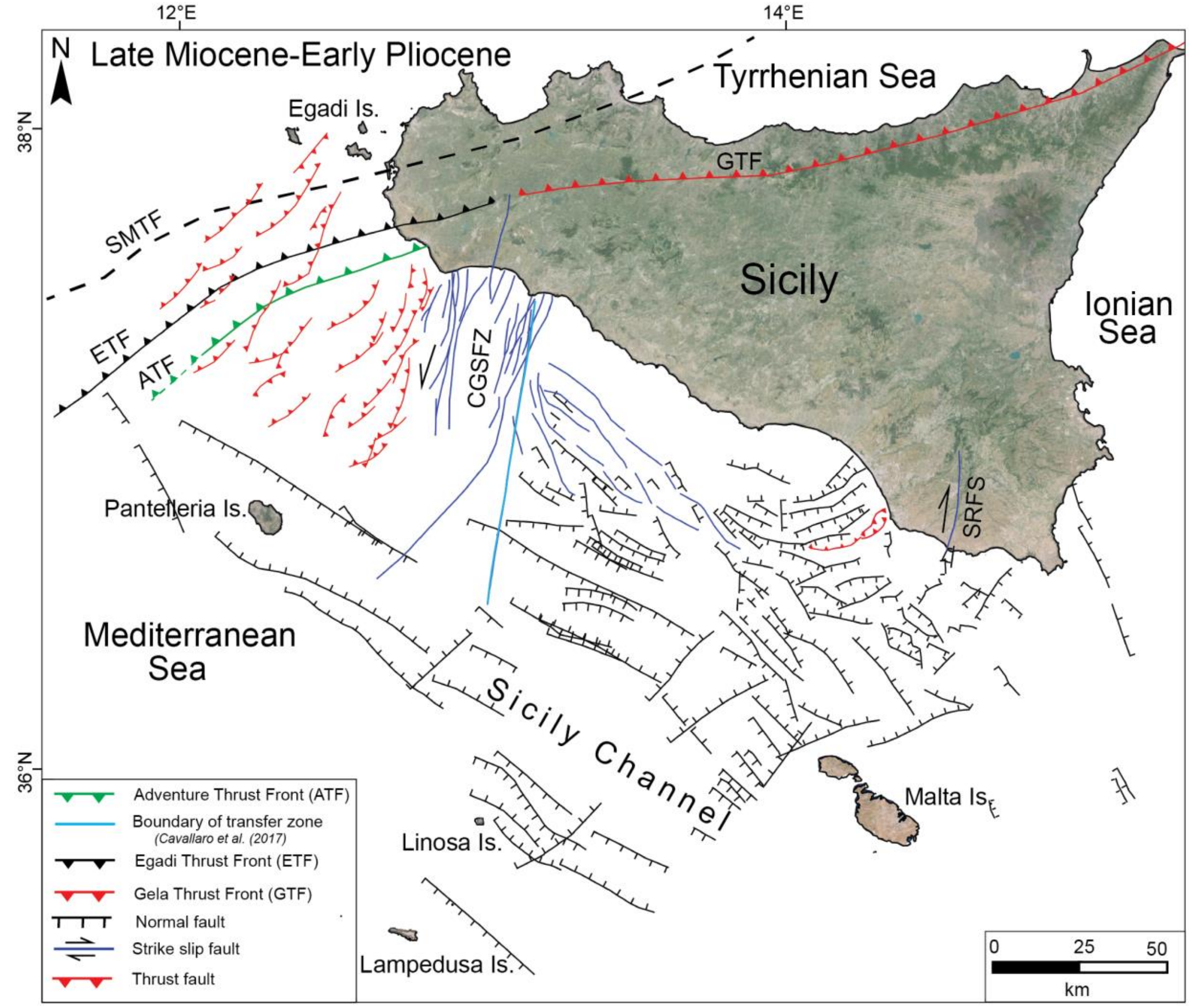
12°E
14°E
38°N
36°N
N
Late Miocene-Early Pliocene
Tyrrhenian Sea
Egadi Is.
GTF
SMTF
ETF
ATF
CGSFZ
Sicily
Ionian Sea
SRFS
Pantelleria Is.
Mediterranean Sea
Sicily Channel
Malta Is.
Linosa Is.
Lampedusa Is.
Adventure Thrust Front (ATF)
Boundary of transfer zone
(Cavallaro et al. (2017)
Egadi Thrust Front (ETF)
Gela Thrust Front (GTF)
Normal fault
Strike slip fault
Thrust fault
0
25
50
km

Figure 15

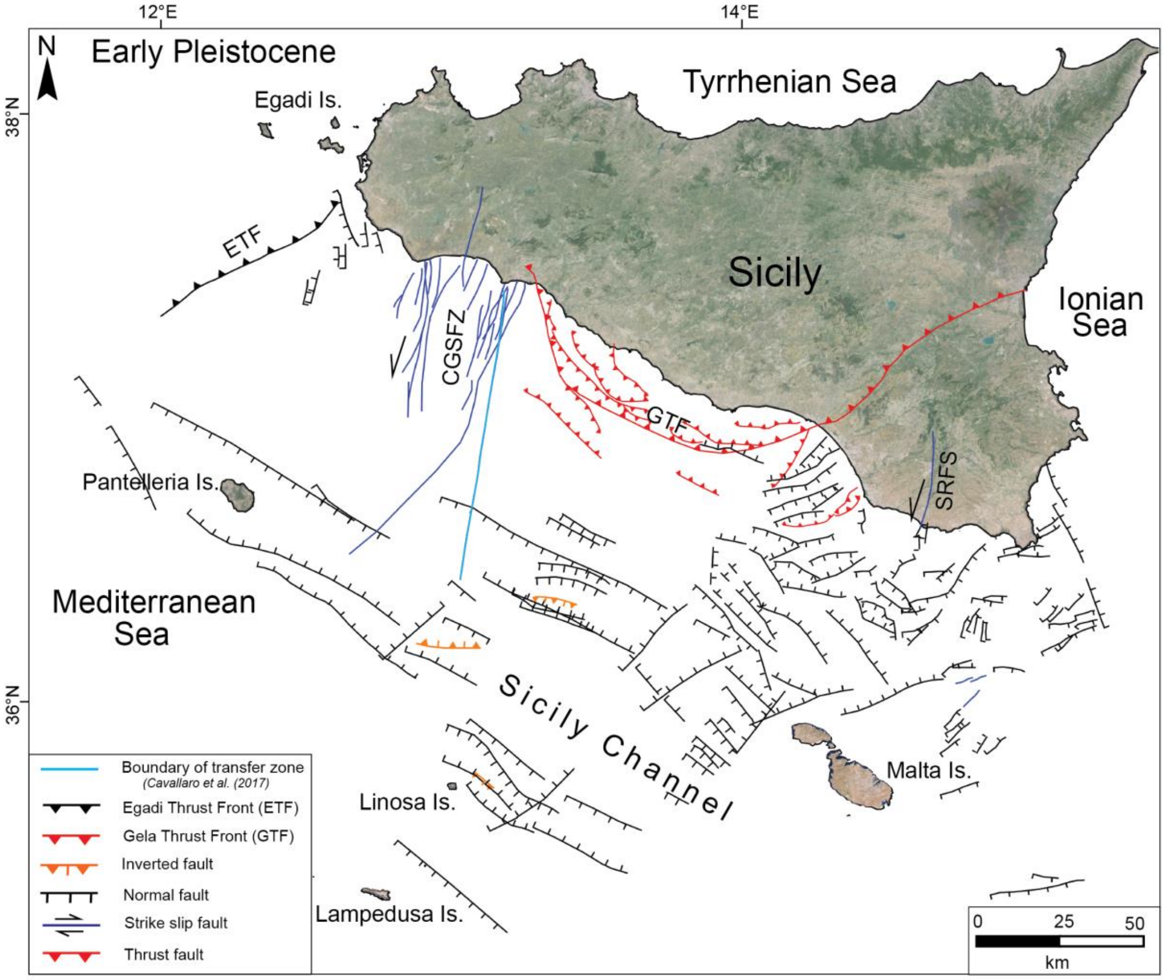
12°E
14°E
38°N
36°N
N
Early Pleistocene
Egadi Is.
Tyrrhenian Sea
ETF
CGSFZ
Sicily
Ionian Sea
GTF
SRFS
Pantelleria Is.
Mediterranean Sea
Sicily Channel
Malta Is.
Linosa Is.
Lampedusa Is.
Boundary of transfer zone
(Cavallaro et al. (2017)
Egadi Thrust Front (ETF)
Gela Thrust Front (GTF)
Inverted fault
Normal fault
Strike slip fault
Thrust fault
0 25 50
km

Figure 16

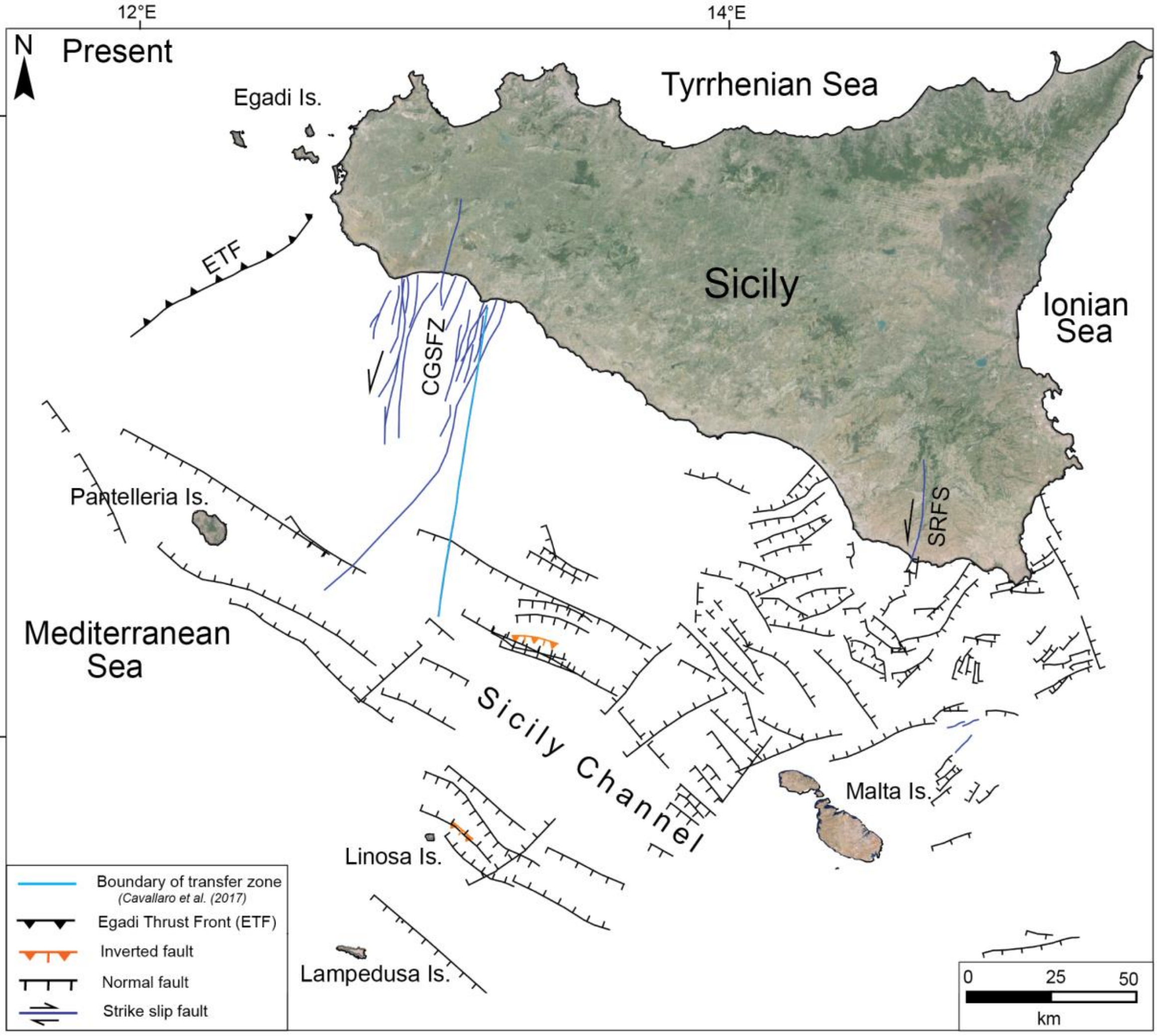
12°E
14°E
38°N
36°N
N
Present
Egadi Is.
Tyrrhenian Sea
ETF
Sicily
Ionian Sea
CGSFZ
Pantelleria Is.
SRFS
Mediterranean Sea
Sicily Channel
Malta Is.
Linosa Is.
Lampedusa Is.
Boundary of transfer zone
(Cavallaro et al. (2017)
Egadi Thrust Front (ETF)
Inverted fault
Normal fault
Strike slip fault
0
25
50
km

Figure 17

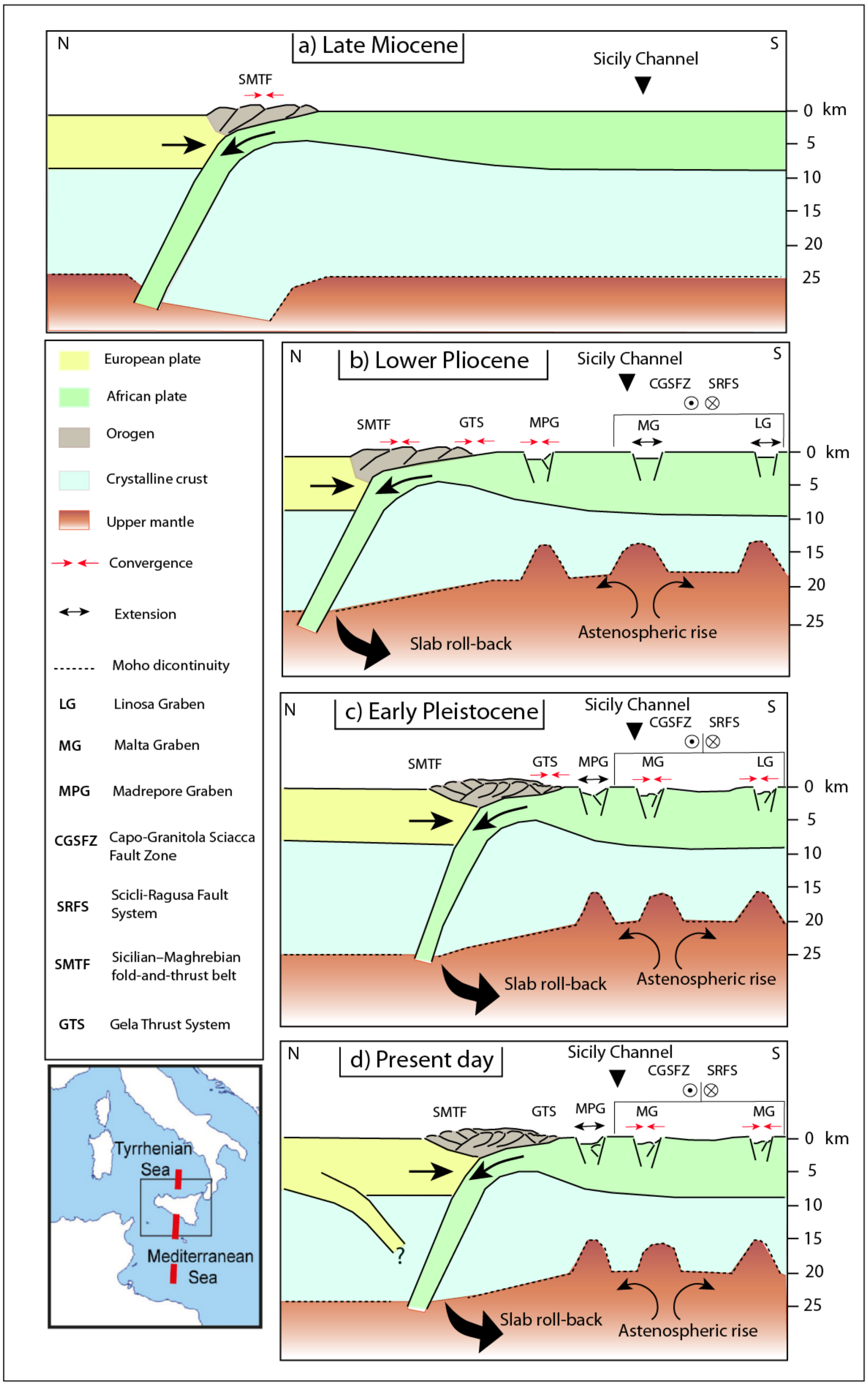
a) Late Miocene
N
S
Sicily Channel
SMTF
0 km
5
10
15
20
25
European plate
African plate
Orogen
Crystalline crust
Upper mantle
Convergence
Extension
Moho dicontinuity
LG
Linosa Graben
MG
Malta Graben
MPG
Madrepore Graben
CGSFZ
Capo-Granitola Sciacca Fault Zone
SRFS
Scicli-Ragusa Fault System
SMTF
Sicilian–Maghrebian fold-and-thrust belt
GTS
Gela Thrust System
b) Lower Pliocene
Sicily Channel
CGSFZ
SRFS
SMTF
GTS
MPG
MG
LG
Slab roll-back
Astenospheric rise
c) Early Pleistocene
Sicily Channel
CGSFZ
SRFS
SMTF
GTS
MPG
MG
LG
Slab roll-back
Astenospheric rise
d) Present day
Sicily Channel
CGSFZ
SRFS
SMTF
GTS
MPG
MG
MG
?
Slab roll-back
Astenospheric rise
Tyrrhenian Sea
Mediterranean Sea

List of tables (Supplementary Materials)

Table 1. Reference, location, and orientation of the seismic lines and well data used in this review.

Line name	**Literature**	**Area covered**	**Orientation**	**Wells used for stratigraphic correlation (ViDEPI database)**
Line 1 (C90-117**)** (Fig. 7a)	Civile et al. (2014)	Adventure Plateau	SE-NW	Samanta-01, Corvina Mare-01, Orlando-01 and Orlando-02
Line 2 (C-1007) (Fig. 8a)	Federik et al. (2018)	Capo Granitola Sciacca Fault Zone	SE-NW	Orione est-01 and Venere-01
Line 3 (C-529) *(Fig. 8b)*	Federik et al. (2018)	Capo Granitola Sciacca Fault Zone	SE-NW	Orione est-01 and Venere-01
Line 4 (Pant-1) (Fig. 9a)	Civile et al. (2021)	Pantelleria Graben	NE-SW	Piera-01, Paola est-01 and Egeria-01Samanta-01, Corvina Mare-01 and Orlando-01
Line 5 (MS120) (Fig. 10a)	Maiorana et al. (2023)	Malta Graben	SSE-NNW	Riccio Sud-01, Remo Nord-01, Palma-01 and Egeria-01
Line 6 (MS119) (Fig. 10b)	Maiorana et al. (2023)	Linosa Graben	SSW-NNE	Riccio Sud-01, Remo Nord-01, Palma-01 and Egeria-01
Line 7 (C-529) (Fig. 10a)	Catalano et al. (1996)	Gela Foredeep Basin	NE-SW	Noemi-01 and Orione-est-01
Line 8 (CS71-SC15) (Fig. 11a)	Cavallaro et al. (2017)	Gela Foredeep Basin	NE-SW	Palma-01 and Egeria-01
Line 9 (CS71-SC17) (Fig.11b)	Cavallaro et al. (2017)	Gela Foredeep Basin	NE-SW	Palma-01 and Egeria-01

Line name	**MS119, MS120**	**Pant-1**	**C90-117**	**CS71-SC17, CS71-SC15**	**C-1007 , C259**
Available in	ViDEPI	OGS	Agip	CNR-ISMAR	ViDEPI
Recording date	1980	2009	1996	1970	1968
Sample rate (ms)	4	2			2
Fold (%)	1200	3000			1200
Recording filters	8-126 Hz	Anti-alias			10-80 Hz
Energy source	Flexotir	Sleeve guns			AquaPulse
Streamer length (m)	2400	1600			1600
Channel	48	120			24
Group interval (m)	50	12.5			67
Shot interval (m)	100	25			137

Table 2. Source and acquisition parameters of the selected seismic lines.

Table 3: Main horizons in the different Sicily Channel sectors investigated in this study.

Area	**Name** *(Acronyms used in this study; Fig. 4)*	**Colour**	**Age (Ma)**	**Description**	**Boundaries and facies**
Adventure Plateau *(Fig. 7a)* Civile et al. (2014) Chronostratigraphy from Samanta-01, Corvina Mare-01, Orlando-01 and Orlando-02 boreholes	Top of Miocene (TMS) Base of Terravechia (BTF) Top of Carbonate succession (TCS)		5.3 11.6 23	The unconformity is probably associated with a Messinian erosional surface that distinguishes the thin layer of the Plio-Quaternary unit and the Miocene section. The base of Tortonian to Messinian succession composed mostly of silty clay and quartz sands. The boundary between predominantly Triassic to Paleogene carbonate succession and the Miocene siliciclastic and carbonate clastic deposits.	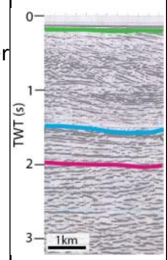
Capo Granitola Sciacca Fault Zone *(Fig. 8a)* Fedorik et al. (2018) Chronostratigraphy from Orione est-01 and Venere-01 boreholes	Top of Miocene succession (TMS) Top of Carbonate (TCS)		5.3 66-34	TMS separates the Plio-Quaternary unit consisting of clays and the Miocene section including Clays with some Marls. TCS separates the upper Miocene unit and the lower Mesozoic carbonates.	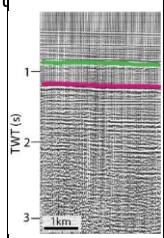
(Fig. 8b) Fedorik et al. (2018) Chronostratigraphy from Orione est-01 and Venere-01 boreholes	Top of Trubi (U1) Top of Miocene (TMS) Top of Carbonate succession (TCS)		3.6 5.3 66-34	U1 is an unconformity, marks a division between the Early Pliocene unit comprising mostly of Marls and the Late Plio-Quaternary unit consisting of Clays. TMS separates the Plio-Quaternary unit (U1) consisting of clays and the Miocene section including Clays with some Marls. TCS separates the upper Miocene unit and the lower Mesozoic carbonates.	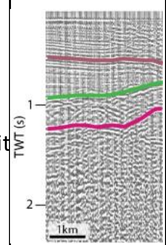
Pantelleria Graben *(Fig. 9a)* Civile et al. (2021) Chronostratigraphy from Piera-01, Paola est-01 and Egeria-01Samanta-01, Corvina Mare-01 and Orlando-01	Top of Calabrian (U3) Top of Trubi (U1) Top of Miocene (TMS) Top of Carbonate succession (TCS)		0.8 3.6 5.3	The sequence is visible on the whole profile and distinguishes the undifferentiated Plio-Quaternary unit seismically. U1 is found in the extreme NE and it divides the Plio-Quaternary syn-rift deposits and the undifferentiated Plio-Quaternary unit. The boundary between siliciclastic Oligocene-Miocene succession and the Plio-Quaternary syn-rift deposits.	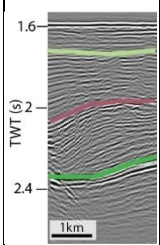

			66-34	Separating the Carbonate platform deposits and the pelagic carbonate succession.	
Malta Graben *(Fig. 10a)* Maiorana et al. (2023)	U2		1.33	The Plio-Pleistocene unit features unconformities (U1 and U2), with a younger extensional event occurring between them. The figure highlights relief affecting the sea floor indicating a contractional phase was or is still active in the graben.	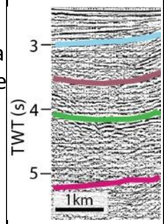
	U1		3.6		
Chronostratigraphy from Riccio Sud-01, Remo Nord-01, Palma-01 and Egeria-01 boreholes	Top of Miocene (TMS)		5.3	The sequence marks the top of Messinian, separates the bottom evaporites and the lower Plio-Pleistocene succession.	
	Top of Carbonate succession (TCS)		66	The boundary between upper cretaceous carbonates and the Miocene unit.	
Linosa Graben *(Fig. 10b)*	U3		0.8	This Upper Calabrian unconformity has sealed the rollover anticline formed by positive inversion.	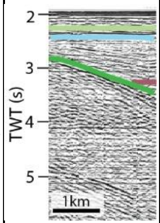
	U2		1.4		
Maiorana et al. (2023)				An extensional phase dated from Zanclean to Calabria with a 0.36 mm/yr sedimentation rate was observed by Syn deposits between U1 and U2.	
Chronostratigraphy from Riccio Sud-01, Remo Nord-01, Palma-01 and Egeria-01 boreholes	U1		4.1		
	Top of Miocene (TMS)		5.3	The boundary between the Messinian evaporites and the lower Plio-Pleistocene succession.	
Gela Foredeep *(Fig. 11a)* Catalano et al. (1996)	Top of Calabrian (U3)		0.8	The unconformity suggests the beginning (Middle Pliocene) and the end (Middle Pleistocene) of the Gela thrust system accretion.	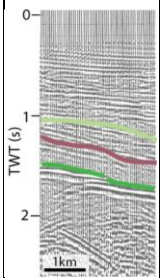
Chronostratigraphy from Noemi-01 and Orione-est-01 boreholes	Top of Trubi (U1)		3.6	The unconformity divides the pelagic marly limestones (Trubi Fm.) from the bottom Messinian evaporites.	
	Top of Miocene (TMS)		5.3	The Messinian reflector divides the Mesozoic carbonates and the evaporites.	

Gela Foredeep *(Fig. 12a)* Cavallaro et al. (2017) Chronostratigraphy from Palma-01 and Egeria-01 boreholes	Top of Miocene (TMS)		5.3	The sequence divides the Messinian evaporite unit and the carbonate and Marl succession of the Oligocene.	
	Top of Ragusa fm. (TR) *(only in Fig. 12a)*		40-23	The sequence represents the top of Ragusa formation in the Maderpore bank and separates the Carbonates and Marls of Oligocene age and middle-upper Miocene silty marls. It appears to correspond to the diffraction hyperbola band.	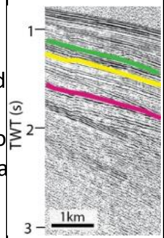
	Top of Carbonate succession (TCS)		66	The sequence is found in the Maderpore bank and marks a boundary between the Jurassic to Lower Miocene carbonate succession and Oligocene to Early Miocene Carbonates and Marls.	
(Fig. 12b) Chronostratigraphy from Palma-01 and Egeria-01 boreholes	Top of Calabrian (U3)		0.8	The depositional sequence boundary refers to the peak of regression in the area.	
	Base of Gelasian (U2)		2.6	The erosional unconformity related to a relative sea-level drop marks a boundary between Zanclean–Piacenzian deposits and the Gelasian to the Calabrian unit.	
	Top of Trubi (U1)		3.6	The base of the Plio-Quaternary unit (U1) interpreted as syn tectonic, distinguishes rhythmically bedded pelagic marly limestones of Trubi formation and the Messinian evaporites.	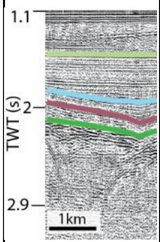
	Top of Miocene (TMS)		5.3	The sequence divides the Messinian evaporite unit and the carbonate and Marl succession of the Oligocene.	